Executive summary of the Thesis entitled Mathematical Modelling of Electrically Conducting Fluid Flow Problems in Presence of Magnetic Field.

A Thesis submitted to

The Maharaja Sayajirao University of Baroda,

Vadodara

For the award of the degree of

Doctor of Philosophy

in

Mathematics

by

MITAL HIREN MISTRY

Under the guidance of

Prof. (Dr.) HARIBHAI R. KATARIA

Dean, Faculty of Science

Professor, Department of Mathematics

The Maharaja Sayajirao University of Baroda, Vadodara- 390002

December 2023

Table of content of Thesis

Table of content of Executive summary of Thesis

Chapter 1

INTRODUCTION AND FUNDAMENTAL CONCEPTS

1.1 Non-Newtonian fluid

Non-Newtonian fluids, such as pastes, gels, polymer solutions, Carreau fluid, William -son fluid, Micropolar fluid, etc., are those that oppose Newton's law of viscosity. Non-Newtonian Fluid is a fluid in which shear stress and rate of shear strain are not linearly related as shown in figure **??**. Blood, grease, honey, shampoo, custard, toothpaste, paint are few examples of non-Newtonian fluids.

1.2 Applications of Non-Newtonian fluid

The study of non-Newtonian fluids is very important since it has many engineering and industrial applications. Such fluids are utilised specifically in the following fields: prescription medications, physiology, material processing, fibre technology, chemical and nuclear industries, oil reservoir engineering, and meals. Shampoos, apple sauce, ketchup, blood at low shear rates, polymer solutions, paints, food items, milk, coating of wires, grease, crystal development, and many more fluids are examples of this type.

1.3 Magnetohydrodynamics

The study of electrically conducting fluid flow in the presence of magnetic field is known as magnetohydrodynamics (MHD).

1.4 Applications of Magnetohydrodynamics

This includes liquid metals like gallium, mercury, and sodium in addition to molten iron. Petroleum, chemical, and metallurgical processing industries provide as the best examples of the significance of MHD fluid flow over a deforming body. Additional real-world applications include surface cooling in technology, wind-up roll processes, and polymer film.

1.5 Magnetohydrodynamics Flow

Magnetohydrodynamics deals with the dynamics of fluids having nonnegligible electrical conductivity which interact with a magnetic field. As a result, motion of an electrically conducting fluid in the presence of a magnetic field, electric current is induced in the fluid. An electrically conducting fluid moving in presence of a magnetic field (transverse) which generate a force called the Lorentz force. This force has a tendency to modify the initial motion of the conducting fluid. Moreover, the induced currents generate their own magnetic field, which is added to the primitive magnetic field. Thus there is an interlocking between the motion of the conductor and the electromagnetic field. The study of MHD has significantly used both in nature and in man-made devices such as cooling of nuclear reactors, metal-working processes, MHD generators, MHD-based micro-coolers, MHD-based stirrer and MHD-based micro-pumps and many more.

1.6 Heat Transfer

Heat transfer is transfer of energy from higher temperature region to lower temperature region, which is because of temperature difference. The basic driving force for heat transfer is temperature variance. This transfer of heat continues till both the regions attains same temperature. Heat transfer issues are involved in different industrial technologies like power engineering, thermal transport etc.

1.6.1 Conduction

It refers to the transfer of heat due to a temperature gradient and by the inter molecular interactions in a stationary medium. In this model of heat transfer, heat flows from a region of higher temperature to a region of lower termperature by kinetic motion or by direct impact of the molecules irrespective of whether the body is at rest or in motion. It takes place in solids, liquids and gases.

1.6.2 Radiation

Transfer of energy through electromagnetic waves is called radiation. It is the only form of heat transfer that can occur in the absence of an intervening medium. Radiation which is emitted by a volume in fluid is due to the thermal agitation of its composing molecules. Transfer of heat by radiation becomes important when the temperature differences are high. It may be noted that radiation also depends on the nature of the fluid.

1.7 Mass Transfer

Mass transfer is the tendency of movement of molecules from one location having high molecule concentration to another location having lower molecule concentration. Mass transfer is one of the most vital characteristics of chemical engineering. The force behind mass transfer is concentration gradient. The mass transfer depends on the diffusion of molecules one phase to another phase and also depends on properties like vapour pressure, concentration etc.

1.8 Governing equations

The laws of conservation of mass, momentum, energy, and mass flux are observed in fluid flows.

1.8.1 Conservation of mass (Equation of continuity)

According to this equation, the excess of mass that flows in over the amount that flows out must match the increase in fluid mass at the surface during any given period of time. This results in the equation of continuity, which can be stated as follows when represented using vector notations:

$$\frac{\partial \rho}{\partial t} + \vec{\nabla} \cdot \left(\rho \vec{V}\right) = 0 \tag{1.8.1}$$

If a fluid's density does not change with pressure, it is said to be incompressible. The continuity equation has the following form when this happens

$$\vec{\nabla} \cdot \vec{V} = 0 \tag{1.8.2}$$

1.8.2 Conservation of Momentum (Equation of Motion)

The second law of motion, which states that the sum of all forces acting on a fluid mass confined in an arbitrary volume fixed in space is equal to the time rate of change in linear momentum, yields the Navier-Stokes equations of motion, which govern the flow behaviour. When represented in vector notation, this law which generates the equation of motion can be written as follows:

$$\rho\frac{D\vec{V}}{Dt} = \rho f_i - \nabla p + \mu\nabla^2\vec{V} \tag{1.8.3}$$

where $\rho\frac{D\vec{V}}{Dt} = \frac{\partial}{\partial t} + \left(\vec{V}\cdot\nabla\right)$ is called the material derivative, ∇^2 is the Laplacian operator, and f_i is the external body forces acting on the enclosed volume.

1.8.3 Conservation of Energy(Equation of Energy)

According to this law, the rate of increase of fluid energy in the volume V is equal to the opposite of the energy's outward flux, plus any energy produced by the body's work, surface forces, thermal conduction, and any other heat sources that may be present.

This law, which results in the equation of energy, can be represented as follows for an incompressible fluid when written in vector notation:

$$\rho C_p\frac{DT}{Dt} = \kappa\nabla^2 T + \frac{\partial Q}{\partial t} + \phi \tag{1.8.4}$$

where ϕ is the heat generated due to friction forces and is usually known as dissipation function.

1.9 Homotopy Analysis Method

Two continuous functions from one topological space to another are called homotopic if one can be continuously deformed into the other, such a deformation is called a homotopy between the two functions.

The basic idea of HAM method [120] is to produce a succession of approximate solutions that tend to exact solution of the problem. Presence of auxiliary parameters and functions in approximate solution, results in production of a family of approximate solutions, rather than a single solution produced by traditional perturbation methods.

The general approach used by HAM is to solve non-linear equation,

$$\mathcal{N}(u(t)) = 0, \quad t > 0, \tag{1.9.1}$$

where $\mathcal{N}$ is a nonlinear operator and $u(t)$ is unknown function of independent variable t.

1.9.1 Zero-order deformation equation

Let $u_0(t)$ denote an initial guess of exact solution of Equation (1.9.1), $\hbar \neq 0$ an auxiliary parameter, $H(t) \neq 0$ auxiliary function and $\mathcal{L}$ an auxiliary linear operator with property,

$$\mathcal{L}(f(t)) = 0 \quad \text{when} \quad f(t) = 0. \tag{1.9.2}$$

The auxiliary parameter $\hbar$, auxiliary function $H(t)$, and auxiliary linear operator $\mathcal{L}$ play important roles within HAM to adjust and control convergence region of solution series. Liao [120] constructs, using $q \in [0, 1]$ as an embedding parameter, so-called zero-order deformation equation,

$$(1-q)\mathcal{L}[\Phi(t;\ q) - u_0(t)] = q\hbar H(t)\mathcal{N}[\Phi(t;\ q)], \tag{1.9.3}$$

where $\Phi(t;\ q)$ is solution which depends on $\hbar$, $H(t)$, $\mathcal{L}$, $u_0(t)$ and q. When $q = 0$, zero-order deformation Equation (1.9.3) becomes,

$$\Phi(t;\ 0) = u_0(t), \tag{1.9.4}$$

when $q = 1$, since $\hbar \neq 0$ and $H(t) \neq 0$, then Equation (1.9.3) reduces to,

$$\mathcal{N}[\Phi(t;\ 1)] = 0. \tag{1.9.5}$$

So, $\Phi(t;\ 1)$ is exactly solution of nonlinear Equation (1.9.1). Expanding $\Phi(t;\ q)$ in Taylor's series with respect to q, we have

$$\Phi(t;\ q) = u_0(t) + \sum_{m=1}^{\infty} q^m u_m(t), \tag{1.9.6}$$

where,

$$u_m(t) = \frac{1}{m!} \left. \frac{\partial^m \Phi(t;\ q)}{\partial q^m} \right|_{q=0}. \tag{1.9.7}$$

If power series (1.9.6) of $\Phi(t;\ q)$ converges at $q = 1$, then we get following series

solution,

$$u(t) = u_0(t) + \sum_{m=1}^{\infty} u_m(t), \tag{1.9.8}$$

where terms $u_m(t)$ can be determined by so-called high-order deformation equations which are described below.

1.9.2 High-order deformation equation

Define vector

$$\vec{u_n} = \{u_0(t), u_1(t), u_2(t), ..., u_n(t)\}. \tag{1.9.9}$$

Differentiating Equation (1.9.3) m times with respect to embedding parameter q, then setting $q = 0$ and dividing them by $m!$, we have so-called m^{th}-order deformation equation,

$$\mathcal{L}\left[u_m(t) - \chi_m u_{m-1}(t)\right] = \hbar H(t)\mathcal{R}_m\left(\vec{u_m}, t\right), \tag{1.9.10}$$

where

$$\chi_m = \begin{cases} 0, & m \leq 1, \\ 1, & otherwise \end{cases} \tag{1.9.11}$$

$$\mathcal{R}_m\left(\vec{u_{m-1}},\ t\right) = \frac{1}{(m-1)!}\frac{\partial^{m-1}\mathcal{N}\left[\Phi(t;\ q)\right]}{\partial q^{m-1}}\bigg|_{q=0}. \tag{1.9.12}$$

For any given nonlinear operator $\mathcal{N}$, term $\mathcal{R}_m\left(\vec{u_{m-1}}, t\right)$ can be easily expressed by Equation (1.9.12). Thus, we can gain $u_1(t)$, $u_2(t)$... by means of solving linear high-order deformation Equation (1.9.10) one after other in order. m^{th}-order approximation of $u(t)$ is given by,

$$u(t) = \sum_{k=0}^{m} u_k(t). \tag{1.9.13}$$

Liao [120] points out that so-called generalized Taylor's series provides a way to control and adjust convergence region through an auxiliary parameter $\hbar$ such that homotopy analysis method is particularly suitable for problems with strong nonlinearity. Abbasbandy [111] gives meaning of auxiliary parameter $\hbar$, and hence uncovers essence of generalized Taylor's expansion as kernel of homotopy analysis method.

1.9.3 Convergence analysis

One of chief aims of HAM method is to produce solutions that will converge in a much larger region than solutions obtained with traditional perturbation methods. Solutions obtained using this method depend on our choice of linear operator $\mathcal{L}$, auxiliary function $H(t)$, initial approximation $u_0(t)$ and value of auxiliary parameter $\hbar$.

Choice of base functions influence convergence of solution series significantly. For example, solution may be expressed as a polynomial or as a sum of exponential functions. It is expected that, base functions that more closely mimic behavior of actual solution should provide much better results than base functions whose behavior differs greatly from behavior of actual solution. Choice of a linear operator, auxiliary function, and initial approximation often determines base functions present in solution. Having selected a linear operator, auxiliary function, and an initial approximation, deformation equations can be developed and solved in series solution. Solution obtained in this way, still contains auxiliary parameter $\hbar$. This solution should be valid for a range of values of $\hbar$. In order to determine optimum value of $\hbar$, $\hbar$ curves of solution are plotted. These curves are obtained by plotting partial sums $u_m(t)$ or their first few derivatives evaluated at a particular value of t against parameter $\hbar$. As long as equation (1.9.1) with given initial or boundary conditions has a unique solution, partial sums and their derivatives will converge to correct solution for all values of $\hbar$ for which solution converges. Which means that $\hbar$ curves will be essentially horizontal over range of $\hbar$ for which solution converges. As long as, $\hbar$ is chosen in this horizontal region, solution must converge to actual solution of equation (1.9.1).

1.10 Review of relevent literature

The study of MHD flow of Newtonian fluid and Non-Newtonian fluid is important phenomena in science and technology fields. In this thesis, study of two dimensional MHD flow of different types of Newtonian fluid and Non-Newtonian fluids likes, Carreau fluid, Micropolar fluid and Hybrid Williamson fluid with heat and mass transfer are discussed. The governing equations are convert in system of Non-linear partial differential equations. So, HAM has been applied for solving governing equations. All the problems (related to the thesis) are briefly reviewed here.

The collective effects of these three significant branches of science namely, Fluid dynamics, Thermodynamics and electrodynamics give rise to the topic Magneto-fluid dynamics (MFD) which in the form of definition read as The science of motion

of electrically conducting fluid in the presence of a magnetic field. The study of Magnetohydrodynemics (MHD) flow of Non-Newtonian fluid has various application in science and engineering fields. The set of equations that describe MHD are a combination of the Navier Stokes and Maxwell's equations. Research works in the magneto hydrodynamics have been advanced significantly during the last few decades in natural sciences and engineering disciplines after the pioneer work of Hartmann [49] in liquid metal duct flows under the strong external magnetic field. Recently, the study of MHD flow done by Kumar and Gupta [97], Borrelli et al. [6] and Kataria et al. [44].

The diverse applications of non-Newtonian fluids in engineering and manufacturing processes have recently drawn researchers' attention. These fluids have the characteristic that the connection between stress and deformation rate is nonlinear. Molten polymers, pulps, and Chyme are examples of this type of fluid. Owing to the fact that it has numerous industrial uses, such as the extrusion of polymer sheets, emulsion-coated sheets like photographic films, melts and solutions of high molecular weight polymers, etc. Williamson [110] initially introduced Williamson fluid model in his groundbreaking study on the flow of pseudo-plastic materials. He created a model equation to describe the movement of pseudo-plastic fluids, and an experiment to test this theory.

Carreau fluid model is another category of non-Newtonian fluids. Such a model has applications in manufacturing processes such as aqueous, and melts. The shear thickening and shear thinning properties of many non-Newtonian fluids are also described by this model. Many scholars have dedicated their effort to explore the properties of such models due to the wide range of applications of the Carreau model in technological processes. The behavior of polymer suspensions in many flow issues is compatible with the Carreau fluid. It is an example of a pure viscous fluid whose viscosity varies with the rate of deformation. The fluid viscosity is based on the shear rate in a model created by Carreau et al. [102]. Carreau fluid flow with convective condition addressed by Madhu et al. [78]. Fluids having microstructure and an asymmetrical stress tensor are known as micropolar fluids. In terms of physical representation, they are fluids made up of randomly oriented particles suspended in a viscous medium. These fluids are used to study the movement of colloidal suspensions, brain fluid, lubricants, and liquid crystals. Eringen [9, 10] created the hypothesis of micropolar fluids. Chaudhary and Jha [106] examined MHD Micropolar fluid flow past a vertical plate.

Numerous researchers have acknowledged the importance of studying magnetohydrodynamic (MHD) Natural Convection Flow with Synchronized Heat and Mass

Transfer Due to a Stretching Sheet due to its frequent occurrence in Geophysical and Energy Transfer Problems, which include both Polymer and Metal Sheets. The effect of a uniform transverse magnetic field on the natural convection flow of an electrically conducting fluid past a vertical plate have been discussed by Raptis and Singh [18]. Hossain [70] investigated MHD natural convection fluid flow in the presence of viscous dissipation and Joule heating effects. Öztop et al. [46] scrutinized a numerical analysis on Natural convection flow of entropy optimized MHD fluid with local heat source. Due to the widespread use of magnetohydrodynamic (MHD) flow mixed convection heat transfer of fluid within the boundary layer in industrial technology and geothermal applications, as well as the MHD power production systems, this technology is of great interest. Selimefendigil and Öztop [33] studied numerical study of mixed convection of non-Newtonian power law fluids under the influence of an inclined magnetic field. Chamkha [7] examined effects of chemical reaction in MHD mixed convective flow along a vertical stretching sheet. Later, Akinshilo [3] found mixed convective heat transfer analysis of MHD fluid flow considering radiation effect through vertical porous medium. Also, Cho [25] discovered effect of inclined magnetic field on MHD Mixed convection heat transfer and entropy generation of Cu-water fluid.

Ohmic heating is another name for joule heating. It is a process through which heat is generated when an electric current flows through a conductor. Electric stoves, electric heaters, incandescent light bulbs, electric fuses, electronic cigarettes, thermistors, food processing, and many more industrial and technological activities employ joule heating in various ways. The viscosity of the fluid will absorb energy from the motion of the fluid and convert it into internal energy of the fluid in a viscous fluid flow. It entails warming the fluid. Dissipation, often known as viscous dissipation, is the term used to describe this largely irreversible process. Several applications, including those where considerable temperature increases are seen in polymer manufacturing flows like injection moulding or extrusion at high rates, are of interest for viscous dissipation. Swain et al. [24] examined Viscous dissipation and joule heating effects on MHD flow past a stretching sheet. Daniel et al. [140] scrutinized double stratification effects on unsteady MHD mixed convection flow of fluid with viscous dissipation and Joule heating effects. Characteristics of Joule heating and viscous dissipation on three-dimensional flow of Oldroyd B nanofluid with thermal radiation have been studied by Kumar et al. [55]. Das et al. [116] explored effects of Joule heating and viscous dissipation on MHD mixed convective slip flow over an inclined porous plate.

MHD flow past a heated surface have applications in manufacturing processes

such as the cooling of the metallic plate, nuclear reactor, extrusion of polymers etc. Ali et al. [131] studied effects of thermal radiation and heat generation/absorption in fluid flow regime. Rehman et al. [59] discussed effects of heat generation/absorption on Carreau fluid flow in a thermally stratified medium. Reddy et al. [103] explored radiation and heat generation/absorption on MHD nanofluid flow with heat and mass transfer over an inclined vertical porous plate. Patel et al. [38] discovered MHD Micropolar Nanofluid flow over a Stretching/Shrinking Sheet. Jena et al. [119] studied effect of chemical reaction and heat source/sink on MHD viscoelastic fluid flow over a vertical stretching sheet. Daniel et al. [139] examined the effects of thermal radiation on MHD nanofluid flow over nonlinear stretching sheet. Ramzan et al. [83] found effects of radiative and joule heating effects on the MHD micropolar fluid flow with partial slip and convective boundary condition. Soomro et al. [32] examined effetcs of velocity slip on MHD mixed convection Williamson nanofluid flow along a vertical surface. Kayalvizhi et al. [73] explored effects velocity slip on heat and mass fluxes of MHD flow over a stretching sheet. Ibrahim [137] examined MHD fluid flow past a stretching sheet with convective boundary condition. Nayak et al. [81] studied MHD nanofluid flow over an stretching sheet with convective boundary conditions. Lin et al. [141] studied about the effects of suction or injection on laminar boundary layer flow of power law fluids past a flat surface with magnetic field. Sharma et al. [61] explored Soret and Dufour effetcs on MHD Flow Considering chemical Reaction. Imtiaz et al. [72] scrutinized the flow of viscous fluid by a curved stretching surface with Soret and Dufour effects.

Numerous logical strategies like differential transformation method, least square method, HAM are seen in the writing for tackling the physical and designing issues. For a portion of the previously mentioned issues, mathematical methods have been created to acquire the precise answer for quite a long time. In any case, because of certain limitations, researchers have thought about scientific methodologies as another option. Among the most popular techniques in this area, which is broadly applied in science and designing, is bother procedure. It should be noticed that bother procedure can't be applied to emphatically nonlinear issues, as it unequivocally relies on small/large parameters. There have been developed approaches like Adomian deterioration strategy and variational emphasis technique that do not rely on small/large parameters. The significant hindrance of these techniques is that they can't guarantee the assembly of series arrangement. Then again, HAM proposed by Liao [121] is an overall insightful way to deal with getting series solution for unequivocally nonlinear conditions, which can give us a basic method for guaranteeing the assembly of arrangement series.

Chapter 2

Entropy optimized MHD fluid flow over a vertical stretching sheet

Entropy optimization is used to enhance the system performance. Entropy generation is caused due to heat fluxes, Joule heating and dissipation etc. To increase the productivity of the systems, The entropy optimization of the system need to be decreased. MHD fluid flow research is important because it has numerous engineering applications, including slurry flows, industrial oils and diluted polymer solutions.

2.1 Novelty of the chapter

Purpose of this chapter is to investigate solution of radiation effect on Entropy optimized MHD fluid flow. Such study may find application in thermal energy, cooling of modern electronic systems, geothermal energy systems, and solar power collectors etc.

2.2 Mathematical Formulation of the Problem

Consider steady, laminar, 2D natural convective flow of an electrically conducting, incompressible, MHD fluid past a verticle stretching surface in the existance of velocity slip. Ignoring magnetic Reynolds number and induced magnetic field. Joule heating, viscous dissipation, heat generation/absorption and thermal radiation are taken into account. physical attributes of irreversibility are discussed. Convective boundary conditions put on the boundary. In Figure 2.1, stretching sheet velocity in the direction of x is $U_w(x) = ax$, with initial stretching rate $a > 0$. Magnetic field $\mathcal{B} = B_0$ is applied in the perpendicular direction of the flow. The equations which are governed for all these assumptions, are derived using Boussinesq's approximation. They are as follows. The flow expression satisfies

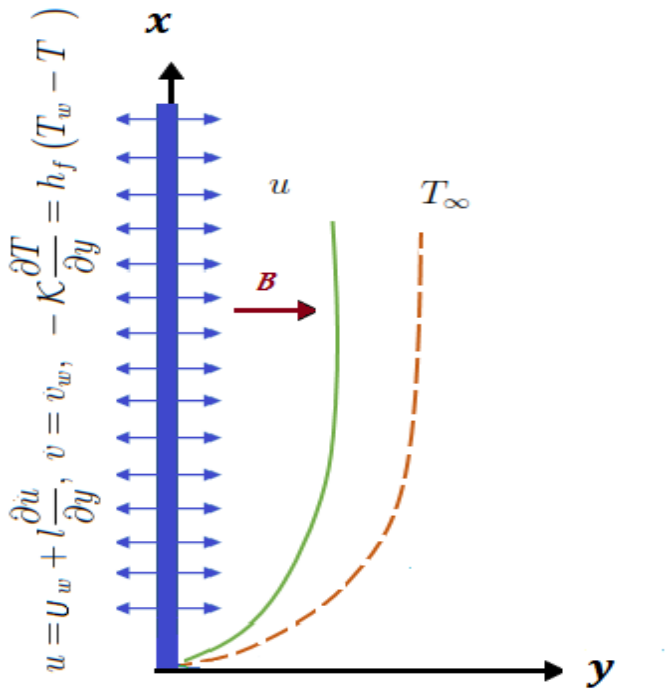

Figure 2.1: Physical sketch

$$\frac{\partial u}{\partial x} + \frac{\partial v}{\partial y} = 0, \tag{2.2.1}$$

$$u\frac{\partial u}{\partial x} + v\frac{\partial u}{\partial y} = \nu\frac{\partial^2 u}{\partial y^2} - \frac{\sigma B_0^2}{\rho}u + g\beta_T(T - T_\infty), \tag{2.2.2}$$

$$\rho C_p\left(u\frac{\partial T}{\partial x} + v\frac{\partial T}{\partial y}\right) = \kappa\frac{\partial^2 T}{\partial y^2} + \mu\left(\frac{\partial u}{\partial y}\right)^2 + \sigma B_0^2 u^2 + Q^*(T - T_\infty) - \frac{\partial q_r}{\partial y}, \tag{2.2.3}$$

with boundary conditions

$$u = U_w + l\frac{\partial u}{\partial y},\ v = v_w,\ -\kappa\frac{\partial T}{\partial y} = h_f(T_w - T) \quad \text{at} \quad y = 0. \tag{2.2.4}$$

$$u \to 0,\ T \to T_\infty \quad \text{as} \quad y \to \infty. \tag{2.2.5}$$

In formulating momentum equation (2.2.2), the ratio of thermal diffusivity to magnetic diffusivity has been kept small when compared to unity. In formulating heat equation (2.2.3), Viscous dissipation is accounted by the term $\frac{\mu}{\rho C_p}\left(\frac{\partial u}{\partial y}\right)^2$, the joule heating is accounted by the term $\frac{\sigma B_0^2 u^2}{\rho C_p}$due to the magnetic field, the value of heat generation/absorption per unit volume is accounted by the term $Q^*(T - T_\infty)$, where Q^* being an inflexible constant, the source term represents the heat generation when

$Q^* > 0$ and the heat absorption when $Q^* < 0$.

Radiative heat flux [126] is:

$$q_r = -\frac{16\sigma^*}{3k^*} T_\infty^3 \frac{\partial T}{\partial y}, \tag{2.2.6}$$

The similarity variable is defined as $\eta = \sqrt{\frac{a}{\nu}} y$ and the stream function is defined as $\psi = \sqrt{a\nu}\, x f(\eta)$.

From η and ψ, we get

$$u = \frac{\partial \psi}{\partial y} = axf'(\eta), \quad v = -\frac{\partial \psi}{\partial x} = -\sqrt{a\nu} f(\eta), \quad \theta(\eta) = \frac{T - T_\infty}{T_w - T_\infty}, \tag{2.2.7}$$

Continuity equation (2.2.1) is satisfied. Equations (2.2.2) and (2.2.3) will reduced in the following form:

$$f''' + Gr_T \theta + ff'' - (f')^2 - Mf' = 0, \tag{2.2.8}$$

$$\left(1 + \frac{4}{3}Rd\right)\theta'' + Prf\theta' + Brf''f'' + MBrf'f' + Pr\beta\theta = 0, \tag{2.2.9}$$

with

$$f(\eta) = f_w, \; f'(\eta) = 1 + \gamma f''(\eta), \theta'(\eta) = -\lambda_1 (1 - \theta(\eta)), \text{ at } \eta = 0,$$
$$f'(\eta) \to 0, \; \theta(\eta) \to 0, \text{ as } \eta \to \infty, \tag{2.2.10}$$

where $Gr_T = \frac{g\beta_T(T_w - T_\infty)}{a^2 x}$, $M = \frac{\sigma B_0^2}{a\rho}$, $Pr = \frac{\mu C_p}{\kappa}$, $Rd = \frac{4\sigma^* T_\infty^3}{3k^*\kappa}$, $f_w = -\frac{v_w}{\sqrt{a\nu}}$, $\gamma = l\sqrt{\frac{a}{\nu}}$, $Ec = \frac{U_w^2}{C_p(T_w - T_\infty)}$, $\beta = \frac{Q^*}{a\rho C_p}$, $\lambda_1 = \sqrt{\frac{\nu}{a}}\frac{h_{ft}}{\kappa}$, $Br = PrEc$.

Velocity gradient is $C_{fx} = \frac{\tau_w}{\rho U_w^2}$, where shear stress $\tau_w = \mu \left(\frac{\partial u}{\partial y}\right)_{y=0}$. Skin friction coefficient is $C_{fx} Re_x^{\frac{1}{2}} = f''(0)$.

Temperature gradient is $Nu_x = \frac{x q_w}{\kappa (T_w - T_\infty)}$, where $q_w = -\kappa \left(1 + \frac{16\sigma^* T_\infty^3}{3\kappa k^*}\right)\left(\frac{\partial T}{\partial y}\right)_{y=0}$ is heat flux at the wall. Nusselt number is $Nu_x Re_x^{-\frac{1}{2}} = -\left(1 + \frac{4}{3}Rd\right)\theta'(0)$, where local Reynold number $Re_x = \frac{xU_w}{\nu}$.

Generation of entropy is

$$S_G = \frac{\kappa}{T_\infty^2}\left(1 + \frac{16\sigma^* T_\infty^3}{3\kappa k^*}\right)\left(\frac{\partial T}{\partial y}\right)^2 + \frac{\mu}{T_\infty}\left(\frac{\partial u}{\partial y}\right)^2 + \frac{\sigma B_0^2}{T_\infty} u^2, \tag{2.2.11}$$

we have entropy generation rate

$$N_G = \alpha_1 \left(1 + \frac{4}{3}Rd\right)\theta'^2 + Brf''^2 + MBrf'^2. \tag{2.2.12}$$

Bejan number is the proportion of heat and mass transfer entropy generation to total entropy generation.

$$Be = \frac{\alpha_1 \left(1 + \frac{4}{3}Rd\right)\theta'^2}{\alpha_1 \left(1 + \frac{4}{3}Rd\right)\theta'^2 + Brf''^2 + MBrf'^2} \tag{2.2.13}$$

where $N_G = \dfrac{T_\infty \nu S_G}{a\kappa(T_w - T_\infty)}$ denotes entropy generation rate, $\alpha_1 = \dfrac{T_w}{T_\infty} - 1$ is temperature difference parameter.

2.3 Solution by Homotopy Analysis Method

Homotopy method is a basic concept of topology. Liao [120] proposed HAM is used in Equations (2.2.8)-(2.2.9) with boundary conditions (2.2.10). Initial guesses $f_0(\eta)$, $\theta_0(\eta)$ and auxiliary linear operators $\mathcal{L}_f$, $\mathcal{L}_\theta$ for the HAM solution can be chosen as

$$f_0(\eta) = f_w + \frac{1}{1+\gamma}\left(1 - e^{-\eta}\right), \theta_0(\eta) = \frac{\lambda_1}{1+\lambda_1}e^{-\eta}, \tag{2.3.1}$$

$$\mathcal{L}_f = \frac{\partial^3 f}{\partial \eta^3} - \frac{\partial f}{\partial \eta}, \mathcal{L}_\theta = \frac{\partial^2 \theta}{\partial \eta^2} + \frac{\partial \theta}{\partial \eta}, \tag{2.3.2}$$

with $\mathcal{L}_f\left(k_1 + k_2 e^{\eta} + k_3 e^{-\eta}\right) = 0$, $\mathcal{L}_\theta\left(k_4 + k_5 e^{-\eta}\right) = 0$, where $k_1, k_2, \ldots, k_5$ are arbitrary constants.

2.3.1 Convergence Analysis

For proper choice of $\hbar_f$ and $\hbar_\theta$, HAM solutions converges. The $f''(0)$ and $\theta'(0)$ functions are plotted to the appropriate approximations to get the allowable values of $\hbar_f$ and $\hbar_\theta$. From Fig. 2.2, we can choose $\hbar_f = -0.94$, $\hbar_\theta = -0.47$.

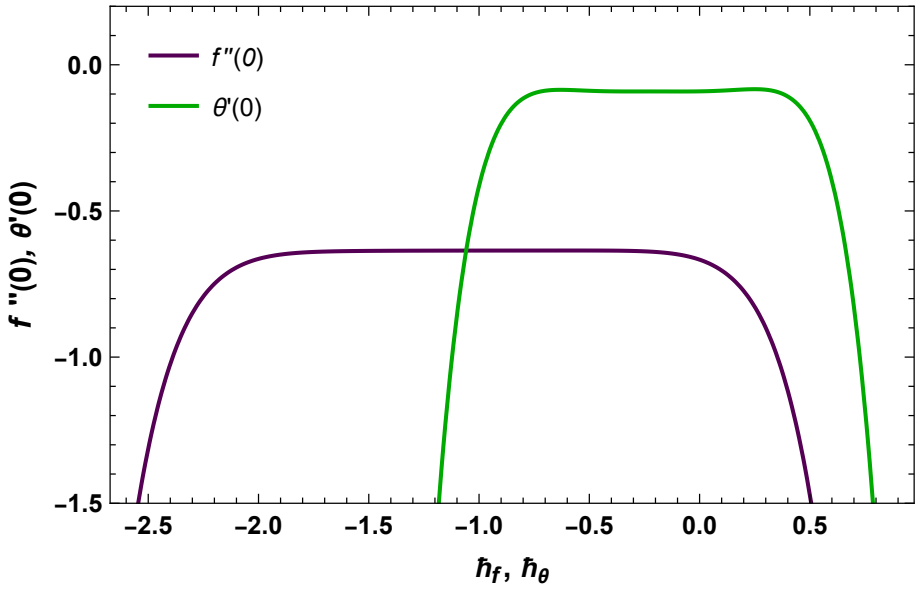

Figure 2.2: $\hbar$-curve for $f''(0),\ \theta'(0)$

2.4 Conclusion

The main findings are:

- M, γ and f_w have similar characteristics for velocity profile.
- Velocity is enhanced against rising amount of Gr_T.
- Rd, M and Br have similar characteristics for temperature profile.
- Temperature is diminished via Pr.
- M, α_1 and Br have similar characteristics for N_G.
- Bejan number has increment for large amount of α_1 and M while decreases for higher values of Br.
- Skin friction coefficient is enhanced via γ and Gr_T and declined via M and f_w.
- Nusselt number is declined against rising values of Br, β and M while behaves opposite for λ_1, Pr and Rd.
- N_G is enhanced via Br, M and α_1 while declined via Rd. Whereas Be is increased via Rd and α_1 while decreased via Br and M, also compared for different values of Pr through tables.

Chapter 3

Effect of nonlinear radiation on MHD fluid flow considering mass transfer

Mass transfer phenomena is found everywhere in nature. The transport of one component in a mixture from a region of higher concentration to one of lower concentration is called mass transfer. Mass transfer finds application in industrial and chemical engineering processes. Such a flow caused by density difference which in turn caused by concentration difference is known as mass transfer flow. Some examples of mass transfer flow are evaporation of water from pond, lake, water reservoir to the atmosphere, separation of chemical species in distillation columns, the diffusion of impurities in rivers, oceans, etc. Radiation plays a significant part in operations involving high temperatures, such as polymer processing, nuclear power plants, glass making, gas turbines, etc.

3.1 Novelty of the Chapter

The main objective of the present work to develop mathematical modelling of heat generation/absorption effects on Entropy optimized MHD fluid flow with mass transfer in the presence of nonlinear radiation. The simplified systems of ordinary differential equations are solve using the Homotopy analysis method.

3.2 Mathematical Formulation of the Problem

Consider steady, two dimensional, incompressible, natural convection MHD flow of electrically conducting fluid with first order velocity slip over vertical stretching sheet as displayed in Figure 3.1. The mathematical model is considered under the

following assumptions and conditions.

- Total entropy subject to heat transfer irreversibility, joule heating irreversibility, viscous dissipation irreversibility and mass diffusion irreversibility are calculated via second law of thermodynamics.
- Induced magnetic field is negligible via small Reynolds number.
- Energy equation mathematically modelled subject to viscous dissipation, joule heating effect, heat generation/absorption and nonlinear radiation.
- Convective boundary condition is applied to the boundary.
- A constant magnetic field of strength $\mathcal{B} = B_0$ is applied in the opposite to the direction of the flow.
- Let us suppose that $u = U_w + U_{Slip} = ax + l\dfrac{\partial u}{\partial y}$ is the stretching velocity with initial stretching rate $a > 0$.

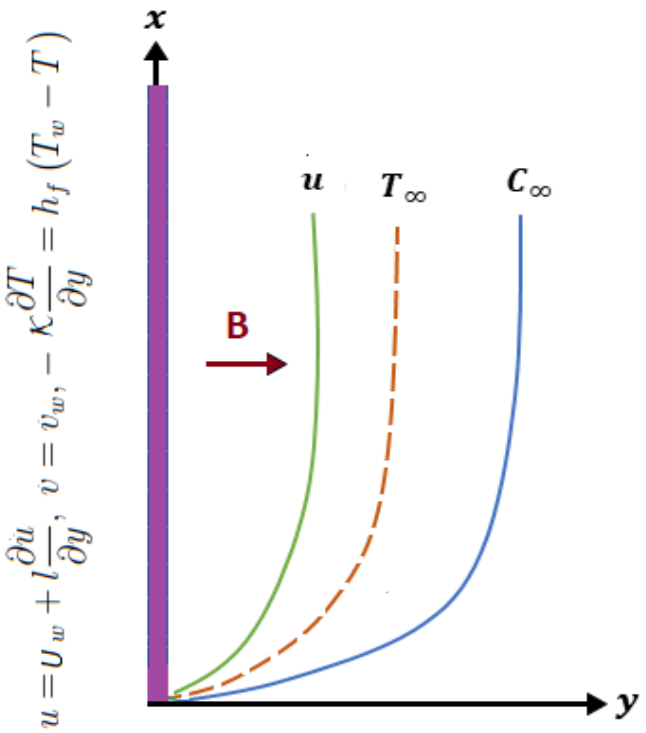

Figure 3.1: Physical sketch

Under the aforementioned assumptions and usual Boussinesq approximations, the governing equations are:

$$\frac{\partial u}{\partial x}+\frac{\partial v}{\partial y}=0, \tag{3.2.1}$$

$$u\frac{\partial u}{\partial x}+v\frac{\partial u}{\partial y}=\nu\frac{\partial^2 u}{\partial y^2}-\frac{\sigma B_0^2}{\rho}u+g\beta_T(T-T_\infty)+g\beta_C(C-C_\infty), \tag{3.2.2}$$

$$\rho C_p\left(u\frac{\partial T}{\partial x}+v\frac{\partial T}{\partial y}\right)=\kappa\frac{\partial^2 T}{\partial y^2}+\mu\left(\frac{\partial u}{\partial y}\right)^2+\sigma B_0^2u^2+Q^*\left(T-T_\infty\right)-\frac{\partial q_r}{\partial y}, \tag{3.2.3}$$

$$u\frac{\partial C}{\partial x}+v\frac{\partial C}{\partial y}=D_M\frac{\partial^2 C}{\partial y^2} \tag{3.2.4}$$

with boundary conditions

$$\left.\begin{array}{l} u=U_w+U_{Slip},\ v=v_w,\ -\kappa\dfrac{\partial T}{\partial y}=h_{ft}\left(T_w-T_\infty\right),\ C=C_w\ \text{ at }\ y=0. \\ u\to 0,\ T\to T_\infty\ C\to C_\infty\ \text{ as }\ y\to\infty. \end{array}\right\} \tag{3.2.5}$$

here first order velocity slip in above boundary condition Eq. 3.2.5 is mathematically expressed as $U_{Slip}=l\dfrac{\partial u}{\partial y}$, where l is free mean molecular path.
Radiative heat flux [126] is:

$$q_r=-\frac{4\sigma^*}{3k^*}\frac{\partial T^4}{\partial y}, \tag{3.2.6}$$

Where σ^* and k^* are the Stefan Stefan-Boltzmann constant and mean absorption coefficient respectively. Now, it can be linearized by considering small temperature differences within the flow such that expanding T^4 with the help of the Taylor series about T_∞ and neglecting higher order terms in the above equation, we get

$$q_r=-\frac{16\sigma^*T_\infty^3}{3k^*}\frac{\partial T}{\partial y}, \tag{3.2.7}$$

The above equation represents to linear thermal radiation, but the intension of the current study is to explore the impact of non-linear thermal radiation, so we replace T_∞^3 with T^3 in Equation (3.2.7)

$$q_r=-\frac{16\sigma^*T^3}{3k^*}\frac{\partial T}{\partial y}, \tag{3.2.8}$$

differentiating equation (3.2.8) with respect to y, we get

$$\frac{\partial q_r}{\partial y}=-\frac{16\sigma^*}{3k^*}\left[3T^2\left(\frac{\partial T}{\partial y}\right)^2+T^3\frac{\partial^2 T}{\partial y^2}\right], \tag{3.2.9}$$

Following similarity transformations are used to covert system of partial differential equations (3.2.1)-(3.2.5), into system of ordinary differential equations

$$\eta = \sqrt{\frac{a}{\nu}}y,\ \psi = \sqrt{a\nu}\ xf(\eta),\quad \theta(\eta) = \frac{T - T_\infty}{T_w - T_\infty},\qquad \phi(\eta) = \frac{C - C_\infty}{C_w - C_\infty}, \tag{3.2.10}$$

where ψ is the stream function, so we get velocity components given as

$$u = \frac{\partial \psi}{\partial y} = axf'(\eta),\ v = -\frac{\partial \psi}{\partial x} = -\sqrt{a\nu}\ f(\eta), \tag{3.2.11}$$

Now using Equations (3.2.9)-(3.2.11), for converting system of partial differential Equations (3.2.1)-(3.2.5) into system of ordinary differential equations, we found continuity equation (3.2.1) is identically satisfied, and dimensionless form of velocity, energy and concentration equations are given as follows:

$$f''' + ff'' - (f')^2 - Mf' + Gr_T\theta + Gr_C\phi = 0, \tag{3.2.12}$$

$$\left[1 + \frac{4}{3}Rd\left\{1 + (\theta_w - 1)\theta\right\}^3\right]\theta'' + 4Rd\left\{1 + (\theta_w - 1)\theta\right\}^2(\theta_w - 1)\theta'^2 + Prf\theta' + Brf''f'' + MBrf'f' + Pr\beta\theta = 0, \tag{3.2.13}$$

$$\phi'' + Scf\phi' = 0, \tag{3.2.14}$$

with

$$f(0) = f_w,\quad f'(0) = 1 + \gamma f''(0),\quad \theta'(0) = -\lambda_1(1 - \theta(0)),\quad \phi(0) = 1 \ \text{ at } \ \eta = 0,$$
$$f'(\eta) \to 0,\ \theta(\eta) \to 0,\ \phi(\eta) \to 0 \ \text{ as } \ \eta \to \infty, \tag{3.2.15}$$

where $Gr_T = \dfrac{g\beta_T(T_w - T_\infty)}{a^2x}$, $Gr_C = \dfrac{g\beta_C(C_w - C_\infty)}{a^2x}$, $M = \dfrac{\sigma B_0^2}{a\rho}$, $Pr = \dfrac{\mu C_p}{\kappa}$, $Rd = \dfrac{4\sigma^* T_\infty^3}{3k^*\kappa}$, $f_w = -\dfrac{v_w}{\sqrt{a\nu}}$, $\gamma = l\sqrt{\dfrac{a}{\nu}}$, $Ec = \dfrac{U_w^2}{C_p(T_w - T_\infty)}$, $\beta = \dfrac{Q^*}{a\rho C_p}$, $\lambda_1 = \sqrt{\dfrac{\nu}{a}}\dfrac{h_{ft}}{\kappa}$, $Sc = \dfrac{\nu}{D_M}$, $\theta_w = \dfrac{T_w}{T_\infty}$, $Br = PrEc$.

The dimensional form of Skin friction coefficient, Nusselt number and Sherwood number are

$$C_{fx} = \frac{\tau_w}{\rho U_w^2}\ ,\ Nu_x = \frac{xq_w}{\kappa(T_w - T_\infty)} \ \text{ and } \ Sh_x = \frac{xq_m}{D_M(C_w - C_\infty)}, \tag{3.2.16}$$

where shear stress $\tau_w = \mu \left(\frac{\partial u}{\partial y}\right)_{y=0}$, heat flux $q_w = -\kappa \left(1 + \frac{16\sigma^* T^3}{3k^*\kappa}\right) \left(\frac{\partial T}{\partial y}\right)_{y=0}$ and mass flux $q_m = -D_M \left(\frac{\partial C}{\partial y}\right)_{y=0}$. So, dimensionless form of physical interest becomes

$$C_{fx} Re_x^{\frac{1}{2}} = f''(0), Sh_x Re_x^{-\frac{1}{2}} = -\phi'(0), \tag{3.2.17}$$

$$Nu_x Re_x^{-\frac{1}{2}} = -\left(1 + \frac{4}{3} Rd \left\{1 + (\theta_w - 1)\theta(0)\right\}^3\right) \theta'(0), \tag{3.2.18}$$

in which $Re_x = \frac{x\, U_w}{\nu}$ shows Reynolds number.

Dimensional form of entropy generation is

$$S_G = \frac{\kappa}{T_\infty^2} \left(1 + \frac{16\sigma^* T^3}{3\kappa k^*}\right) \left(\frac{\partial T}{\partial y}\right)^2 + \frac{\mu}{T_\infty} \left(\frac{\partial u}{\partial y}\right)^2 + \frac{\sigma B_0^2}{T_\infty} u^2 + \frac{RD}{C_\infty} \left(\frac{\partial C}{\partial y}\right)^2, \tag{3.2.19}$$

now, using Equations (3.2.10)-(3.2.11), the dimensionless form is

$$N_G = \alpha_1 \left(1 + \frac{4}{3} Rd \left\{1 + (\theta_w - 1)\theta\right\}^3\right) \theta'^2 + Br f''^2 + MBr f'^2 + \left(\frac{L^*}{\alpha_1}\right) \alpha_2 \phi'^2, \tag{3.2.20}$$

where R is the ideal gas constant, $L^* = \frac{RDC_\infty}{\kappa}$ is diffusion parameter, $\alpha_2 = \left(\frac{C_w - C_\infty}{C_\infty}\right)^2$ is concentration ratio parameter.

$$Be = \frac{\text{Heat and mass transfer irreversibilities}}{\text{Total entropty genearation}} \tag{3.2.21}$$

So mathematical expression of Be is given as

$$Be = \frac{\alpha_1 \left(1 + \frac{4}{3} Rd \left\{1 + (\theta_w - 1)\theta\right\}^3\right) \theta'^2 + \left(\frac{L^*}{\alpha_1}\right) \alpha_2 \phi'^2}{\alpha_1 \left(1 + \frac{4}{3} Rd \left\{1 + (\theta_w - 1)\theta\right\}^3\right) \theta'^2 + Br f''^2 + MBr f'^2 + \left(\frac{L^*}{\alpha_1}\right) \alpha_2 \phi'^2} \tag{3.2.22}$$

3.3 Solution by Homotopy Analysis Method

Homotopy method is a basic concept of topology. Liao [120] proposed HAM is used in Equations (3.2.12)-(3.2.14) with boundary conditions (3.2.15). Initial guesses $f_0(\eta)$, $\theta_0(\eta)$, $\phi_0(\eta)$ and auxiliary linear operators $\mathcal{L}_f$, $\mathcal{L}_\theta$, $\mathcal{L}_\phi$ for the HAM solution

can be chosen as

$$f_0(\eta) = f_w + \frac{1}{1+\gamma}\left(1 - e^{-\eta}\right), \theta_0(\eta) = \frac{\lambda_1}{1+\lambda_1} e^{-\eta}, \phi_0(\eta) = e^{-\eta}, \tag{3.3.1}$$

$$\mathcal{L}_f = \frac{\partial^3 f}{\partial \eta^3} - \frac{\partial f}{\partial \eta}, \mathcal{L}_\theta = \frac{\partial^2 \theta}{\partial \eta^2} + \frac{\partial \theta}{\partial \eta}, \mathcal{L}_\phi = \frac{\partial^2 \phi}{\partial \eta^2} + \frac{\partial \phi}{\partial \eta} \tag{3.3.2}$$

with $\mathcal{L}_f\left(k_1 + k_2 e^{\eta} + k_3 e^{-\eta}\right) = 0$, $\mathcal{L}_\theta\left(k_4 + k_5 e^{-\eta}\right) = 0$, $L_\phi\left(k_6 + k_7 e^{-\eta}\right) = 0$, where $k_1, k_2, \ldots, k_7$ are arbitrary constants.

3.3.1 Convergence Analysis

The solution of the convergence rate in the HAM method depends strongly on parameter $\hbar$. The $f''(0)$, $\theta'(0)$ and $\phi'(0)$ functions are plotted at the 20^{th}-order of approximations to get the allowable values of $\hbar_f$, $\hbar_\theta$ and $\hbar_\phi$. The values of $\hbar_f$, $\hbar_\theta$ and $\hbar_\phi$ are selected in such a way that curves are parallel to $\hbar$-axis. From Figures 3.2-?? we can choose $\hbar_f = -1.51$, $\hbar_\theta = -0.22$ and $\hbar_\phi = -0.88$.

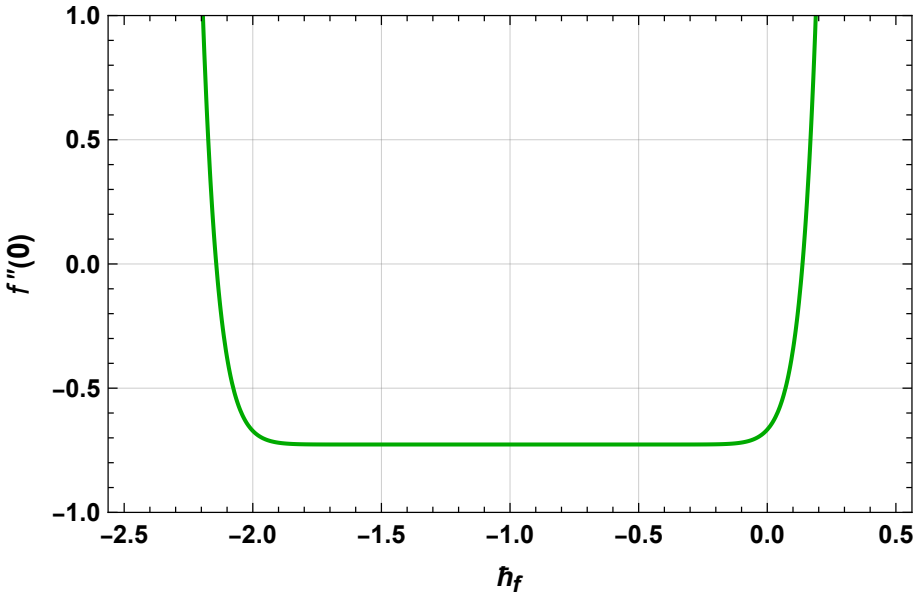

Figure 3.2: $\hbar$-curve for $f''(0)$

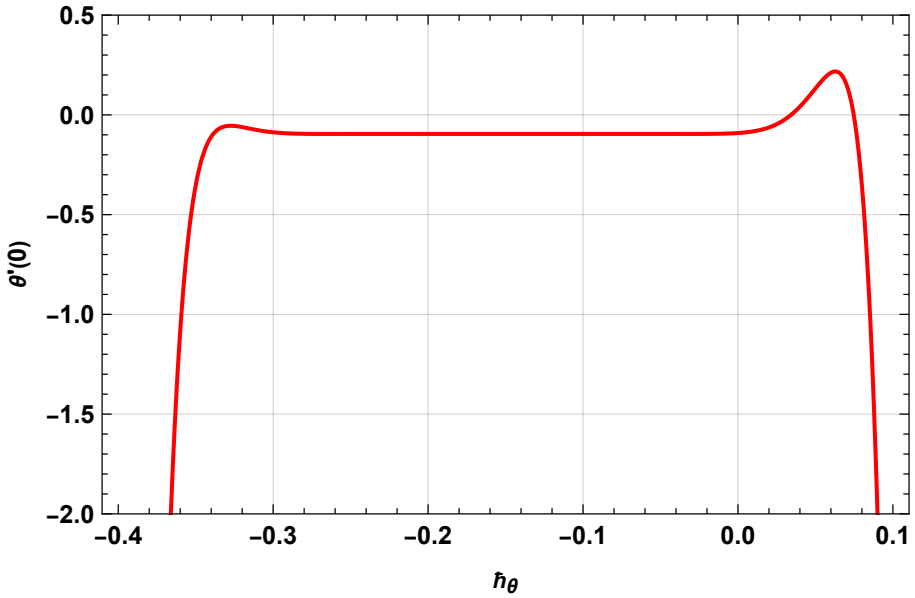

Figure 3.3: $\hbar$-curve for $\theta'(0)$

3.4 Conclusion

Our motive of the present study is to investigate entropy optimisation of 2D Steady, incompressible, Natural convection MHD flow of electrically conducting fluid over vertical stretching sheet in the presence of first-order velocity slip. The problem is solved using HAM. The major findings of this study are

- Velocity reduces compared to rising M, γ and f_w values.
- Temperature declines with increase in Pr, while enhances with increase in Rd, θ_w and Br.
- For larger Sc and f_w values, concentration decreases.
- N_G augmented when increment occurs in M, L^* and Br.
- Br and L^* have opposite effect on Bejan number.
- Be declines with increase in M when $\eta < 1$, for $\eta > 1$, Be enhanced.
- Skin friction coefficient enhances via γ and Gr_T.
- Nusselt number enhances against rising values of Pr, θ_w and Rd.
- Skin friction coefficient and Sherwood number have opposite behaviour for f_w.

Chapter 4

Soret and Dufour impact on MHD Williamson fluid flow with varying viscosity

Williamson fluid is characterized as a non-Newtonian fluid with shear thinning property i.e., viscosity decreases with increasing rate of shear stress. Chyme in small intestine is one of the example of Williamson fluid. The temperature of the fluid as well as the nature of the fluid have a major impact on viscosity. The viscosity should be a temperature dependant variable rather than a constant at high temperatures. When calculating the surface calculating factors, the assumption of constant viscosity causes measurably inaccurate results.

4.1 Novelty of the Chapter

To the best of the knowledge, till date there are no attempts to model, no investigation has been made which provides the analytic expression for the steady two-dimensional MHD Williamson fluid flow over stretching sheet considering the effect of heat generation/absorption, nonlinear radiation and variable viscosity. Homotopy analysis method [120] is used for finding solutions of the governing equations.

4.2 Mathematical Formulation of the Problem

Figure 4.1 shows incompressible MHD Williamson fluid flow past a stretching sheet. It is assumed that the sheet is stretching with the plane $y = 0$ and that the flow is constrained to $y > 0$. In the scenario where $a > 0$ is constant and the x-axis is estimated along the extending surface, with stretching velocity $u(x) = ax$. A uniform magnetic field that is applied perpendicular to an expanding sheet.
The governing equations for Williamson fluid are:

$$\nabla \cdot V = 0 \tag{4.2.1}$$

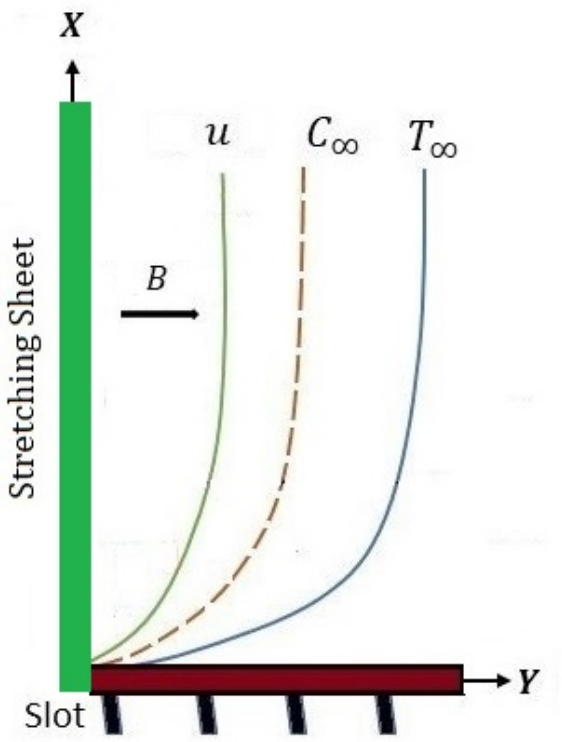

Figure 4.1: Physical problem

$$\rho\frac{dV}{dt} = \nabla\cdot S + F_L + \rho\left\{g\beta_C(C-C_\infty) + g\beta_T(T-T_\infty)\right\} \tag{4.2.2}$$

$$\rho C_p\frac{dT}{dt} = \nabla\cdot(\kappa\nabla T) + Q^*(T-T_\infty) - \nabla q_r + \nabla\cdot\left\{\frac{\rho D_M K_T}{C_s}\right\}\nabla C \tag{4.2.3}$$

$$\frac{dC}{dt} = \nabla\cdot\{D_M\nabla C\} + \nabla\cdot\left\{\frac{D_M K_T}{T_m}\nabla T\right\} \tag{4.2.4}$$

where V is velocity vector and $\frac{d}{dt}$ represents material time derivative.

The governing equations for Williamson fluid are:

$$\frac{\partial u}{\partial x} + \frac{\partial v}{\partial y} = 0, \tag{4.2.5}$$

$$u\frac{\partial u}{\partial x} + v\frac{\partial v}{\partial y} = \frac{1}{\rho}\frac{\partial}{\partial y}\left(\mu(T)\frac{\partial u}{\partial y}\right) + \frac{\Gamma}{\sqrt{2}\rho}\frac{\partial}{\partial y}\left[\mu(T)\left(\frac{\partial u}{\partial y}\right)^2\right] - u\frac{\sigma B^2}{\rho} + g\beta_C(C-C_\infty) + g\beta_T(T-T_\infty), \tag{4.2.6}$$

$$u\frac{\partial T}{\partial x} + v\frac{\partial T}{\partial y} = \frac{\kappa}{\rho C_p}\frac{\partial^2 T}{\partial y^2} + \frac{\rho D_M K_T}{C_s}\frac{\partial^2 C}{\partial y^2} + Q^*(T-T_\infty) - \frac{1}{\rho C_p}\frac{\partial q_r}{\partial y}, \tag{4.2.7}$$

$$u\frac{\partial C}{\partial x} + v\frac{\partial C}{\partial y} = \frac{D_M K_T}{T_m}\frac{\partial^2 T}{\partial y^2} + D_M\frac{\partial^2 C}{\partial y^2}, \tag{4.2.8}$$

with

$$u = U_w = ax, \quad v = 0, \; C = C_w, \quad T = T_w \text{ at } \; y = 0, \tag{4.2.9}$$

$$u \to 0, \quad C \to C_\infty, \quad T \to T_\infty \; \text{ at } \; y \to \infty. \tag{4.2.10}$$

Linearized Heat flux [126] is:

$$q_r = -\frac{16\sigma^*}{3k^*} T_\infty^3 \frac{\partial T}{\partial y} \tag{4.2.11}$$

For the significance of non-linear thermal radiation, we convert T_∞^3 with T^3 in the equation (4.2.11),

$$q_r = -\frac{16\sigma^*}{3k^*} T^3 \frac{\partial T}{\partial y} \tag{4.2.12}$$

then,

$$\frac{\partial q_r}{\partial y} = -\frac{16\sigma^*}{3k^*} \left[3T^2 \left(\frac{\partial T}{\partial y} \right)^2 + T^3 \frac{\partial^2 T}{\partial y^2} \right] \tag{4.2.13}$$

The temperature dependent viscosity by Ajayi et al. [127] is

$$\mu(T) = \; \mu^* \left[1 + b \left(T_w - T \right) \right], \text{ where } b > 0. \tag{4.2.14}$$

Introducing the following transformation to convert equations (4.2.5)-(4.2.10),

$$\psi = x\sqrt{a\nu} f(\eta), \quad \eta = \sqrt{a/\nu} y, \; u = axf'(\eta), \quad v = -\sqrt{a\nu} f(\eta), \tag{4.2.15}$$

$$C = C_\infty + (C_w - C_\infty)\phi(\eta), \quad T = T_\infty + (T_w - T_\infty)\theta(\eta). \tag{4.2.16}$$

Using above transformations, equations (4.2.6-4.2.10) become :

$$(1 + \zeta - \zeta\theta) f'''(1 + 2Wef'') - \zeta(1 + Wef'') f''\theta' + ff'' - Mf' + Gr_T\theta + Gr_C\phi - f'f' = 0 \tag{4.2.17}$$

$$\left(1 + \frac{4}{3} Rd \left\{ 1 - (1 - \theta_w)\theta \right\}^3 \right) \theta'' + 4Rd \left\{ (1 - \theta_w)\theta - 1 \right\}^2 (1 - \theta_w)\theta'^2 + DuPr\phi'' + \beta Pr\theta + Prf\theta' = 0 \tag{4.2.18}$$

$$\phi'' + Sc\phi' f + SrSc\theta'' = 0 \tag{4.2.19}$$

with

$$f(0) = \; \phi(\infty) = \; f'(\infty) = \; \theta(\infty) = \; \; 0, \; f'(0) = \; \phi(0) = \; \theta(0) = \; 1. \tag{4.2.20}$$

Skin friction factor, rate of heat and mass transfer at the wall are respectively

$$C_f = \frac{\tau_w}{\rho U_w^2}, Nu = \frac{xq_w}{\kappa(T_w - T_\infty)}, Sh = \frac{xq_m}{D_M(C_w - C_\infty)} \tag{4.2.21}$$

At the wall, τ_w, q_m and q_w denote the skin stress, diffusion of mass and heat, where

τ_w, q_m and q_w defined in the following

$$\tau_w = \mu u_y \left[1 + \Gamma u_y\right]_{y=0}, \quad q_m = -D_M \left[C_y\right]_{y=0}, \quad q_w = -\kappa \left(1 + \frac{16\sigma^* T^3}{3k^*\kappa}\right) \left[T_y\right]_{y=0}. \tag{4.2.22}$$

using similarity variables, Skin friction factor, Sherwood and Nusselt numbers

$$\left.\begin{aligned} C_f \left(Re_x^{\frac{1}{2}}\right) &= (1 + \zeta - \zeta\theta)\, f''(0) \left[1 + We f''(0)\right], \\ ShRe_x^{-\frac{1}{2}} = -\phi'(0), \quad NuRe_x^{-\frac{1}{2}} &= -\left(1 + \tfrac{4}{3} Rd \left\{1 + (\theta_w - 1)\theta\right\}^3\right) \theta'(0), \end{aligned}\right\} \tag{4.2.23}$$

where $Re_x^{\frac{1}{2}} = \sqrt{\frac{a}{\nu}} x$.

4.3 Solution by Homotopy Analysis Method

Initial guesses and auxiliary linear operators are respectively

$$f_0(\eta) = 1 - e^{-\eta}, , \quad \theta_0(\eta) = e^{-\eta}, \quad \phi_0(\eta) = e^{-\eta}, \tag{4.3.1}$$

$$\mathcal{L}_f = \frac{\partial^3 f}{\partial \eta^3} - \frac{\partial f}{\partial \eta}, \ \mathcal{L}_\theta = \frac{\partial^2 \theta}{\partial \eta^2} + \frac{\partial \theta}{\partial \eta}, \ \mathcal{L}_\phi = \frac{\partial^2 \phi}{\partial \eta^2} + \frac{\partial \phi}{\partial \eta}, \tag{4.3.2}$$

with $\mathcal{L}_f \left(k_1 + k_2 e^{\eta} + k_3 e^{-\eta}\right) = 0$, $\mathcal{L}_\theta \left(k_4 + k_5 e^{-\eta}\right) = 0$, $\mathcal{L}_\phi \left(k_6 + k_7 e^{-\eta}\right) = 0$, where k_i, $i = 1, 2, ..., 7$ are arbitrary constants.

4.3.1 Convergence Analysis

Solutions for HAMs are highly dependent on values for auxiliary parameters $\hbar_f$, $\hbar_\theta$ and $\hbar_\phi$ that influence convergence and approximation rates. As a result, the Figures 4.2, **??** show corresponding $\hbar$-curves taking 20^{th} HAM approximation. For the values $\hbar_f = -1.09$, $\hbar_\theta = -0.75$ and $\hbar_\phi = -0.83$, we get convergence of the series.

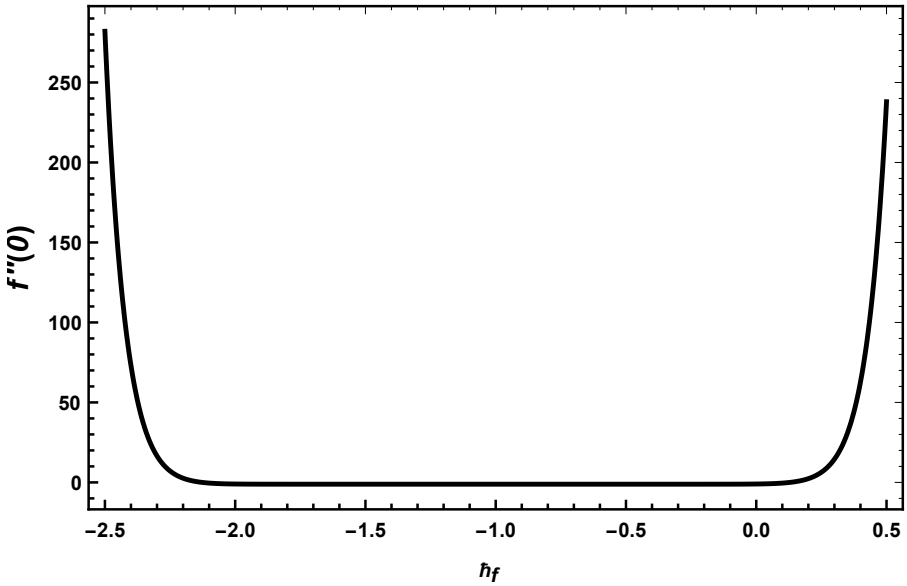

Figure 4.2: $\hbar$-curve for $f''(0)$

4.4 Conclusion

The intention of current research is to explore and compare the combined impacts of temperature dependent viscosity, Soret and Dufour effects on natural convective flow of MHD Williamson fluid past a stretching sheet. The main findings of the research are following:

- We and M reduce velocity profile while Gr_T, Gr_C and ζ behave in opposite way.
- A rise in temperature is observed for M, β, and Du, while a decline is observed for Pr.
- Temperature profile increased for Radiation parameter and temperature ratio parameter.
- Sc and Sr have opposite characteristics according to the concentration profile.
- Skin friction factor is enhanced for We, Gr_T and Gr_C whereas declined for M and ζ.
- Nusselt number is increased for M, Gr_T, Pr, Rd and θ_w while decreased for Du and β.
- Sherwood number is raised for Sc but decayed for Sr.

Chapter 5

MHD Carreau fluid flow over nonlinear stretching sheet

Mathematically, the non-Newtonian behaviour of blood in narrow arteries is examined by treating the blood as a Carreau fluid. Stretching a sheet facilitates heat and mass transfer, which has numerous applications in the polymer sector, including lamination, spinning fibres, and other processes.

5.1 Novelty of the Chapter

Purpose of this chapter is to investigate analytic solution of Soret and Duour effects on MHD Carreau fluid flow over stretching/Shrinking sheet considering variable visocity. Solution of the problem is found by Homotopy analysis method.

5.2 Mathematical Formulation of the Problem

Consider $2D$ steady, incompressible MHD Carreau fluid flow over a shrinking or stretching sheet is considered. Stretching/shrinking sheet is taken along x axis. Magnetic field $\mathcal{B} = B_0 x^{\frac{m-1}{2}}$ is implemented perpendicular to the surface, where $U_w(x) = a^* x^m$ and $U_e(x) = b^* x^m$. Non-linear thermal radiation, Soret and Dufour effects are taken into account.
The basic equations of MHD are given by

$$\nabla \cdot V = 0, \tag{5.2.1}$$

$$\rho \frac{dV}{dt} = \nabla \cdot S + F_L \tag{5.2.2}$$

$$\left(\frac{dT}{dt}\right) = \frac{1}{\rho C_p} \nabla \cdot (\kappa \nabla T) - \frac{1}{\rho C_p} \nabla \cdot q_r + \nabla \cdot \left(\frac{D_M K_T}{C_p C_s} \nabla C\right), \tag{5.2.3}$$

$$\frac{dC}{dt} = \nabla \cdot (D_M \nabla C) + \nabla \cdot \left(\frac{D_M K_T}{T_m} \nabla T\right), \tag{5.2.4}$$

Now, Continuity Eq. (5.2.1) simplified as:

$$\frac{\partial u}{\partial x}+\frac{\partial v}{\partial y}=0, \tag{5.2.5}$$

Now, stress tensors are given as

$$\tau_{xx}=2\mu^*\frac{\partial u}{\partial x}\left(1+\Gamma^2\left(\frac{p_i-1}{2}\right)\left(\frac{\partial u}{\partial y}\right)^2\right),\quad \tau_{yy}=2\mu^*\frac{\partial v}{\partial y}\left(1+\Gamma^2\left(\frac{p_i-1}{2}\right)\left(\frac{\partial u}{\partial y}\right)^2\right), \tag{5.2.6}$$

$$\tau_{yx}=\tau_{xy}=\mu^*\left(\frac{\partial u}{\partial y}+\frac{\partial v}{\partial x}\right)\left(1+\Gamma^2\left(\frac{p_i-1}{2}\right)\left(\frac{\partial u}{\partial y}\right)^2\right). \tag{5.2.7}$$

then,

$$\begin{aligned}\rho\left(u\frac{\partial u}{\partial x}+v\frac{\partial u}{\partial y}\right)&=-\frac{\partial P}{\partial x}+\frac{\partial \tau_{xy}}{\partial y}+\frac{\partial \tau_{xx}}{\partial x}-\sigma\mathcal{B}^2u,\\ \rho\left(u\frac{\partial v}{\partial x}+v\frac{\partial v}{\partial y}\right)&=-\frac{\partial P}{\partial y}+\frac{\partial \tau_{yy}}{\partial y}+\frac{\partial \tau_{yx}}{\partial x},\end{aligned} \tag{5.2.8}$$

In polar coordiantes, Eq. (5.2.2) simplified as below,

$$\begin{aligned}u\frac{\partial u}{\partial x}+v\frac{\partial u}{\partial y}=\frac{1}{\rho}\frac{\partial}{\partial y}\left(\mu^*(T)\frac{\partial u}{\partial y}\right)-\frac{1}{\rho}\frac{\partial P}{\partial x}+3\frac{\mu^*(T)}{\rho}\left(\frac{p_i-1}{2}\right)\Gamma^2\left(\frac{\partial u}{\partial y}\right)^2\frac{\partial^2u}{\partial y^2}\\ +\frac{1}{\rho}\left(\frac{p_i-1}{2}\right)\Gamma^2\frac{\partial\mu^*(T)}{\partial y}\left(\frac{\partial u}{\partial y}\right)^3-\frac{\sigma\mathcal{B}^2}{\rho}u,\end{aligned} \tag{5.2.9}$$

because the flow field is uniform at a suitably large distance from the edge surface, so in the free stream $u=U_e=b^*x^m$, then the Eq. (5.2.9) reduced to

$$\frac{1}{\rho}\frac{\partial P}{\partial x}=-U_e\frac{dU_e}{dx}-\frac{\sigma\mathcal{B}^2}{\rho}U_e, \tag{5.2.10}$$

eliminating $\frac{\partial P}{\partial x}$ in Eq. (5.2.9) by using Eq. (5.2.10), we finally obtain

$$\begin{aligned}u\frac{\partial u}{\partial x}+v\frac{\partial u}{\partial y}=U_e\frac{dU_e}{dx}+\frac{\sigma\mathcal{B}^2}{\rho}U_e+\frac{1}{\rho}\frac{\partial}{\partial y}\left(\mu^*(T)\frac{\partial u}{\partial y}\right)+3\frac{\mu^*(T)}{\rho}\left(\frac{p_i-1}{2}\right)\Gamma^2\left(\frac{\partial u}{\partial y}\right)^2\frac{\partial^2u}{\partial y^2}\\ +\frac{1}{\rho}\left(\frac{p_i-1}{2}\right)\Gamma^2\frac{\partial\mu^*(T)}{\partial y}\left(\frac{\partial u}{\partial y}\right)^3-\frac{\sigma\mathcal{B}^2}{\rho}u,\end{aligned} \tag{5.2.11}$$

reduced form of energy and concentration equations (5.2.3) and (5.2.4) are

$$u\frac{\partial T}{\partial x}+v\frac{\partial T}{\partial y}+\frac{1}{\rho C_p}\frac{\partial q_r}{\partial y}-\frac{\kappa}{\rho C_p}\frac{\partial^2T}{\partial y^2}-\frac{D_MK_T}{C_pC_s}\frac{\partial^2C}{\partial y^2}=0, \tag{5.2.12}$$

$$u\frac{\partial C}{\partial x}+v\frac{\partial C}{\partial y}-\frac{D_M K_T}{T_m}\frac{\partial^2 T}{\partial y^2}-D_M\frac{\partial^2 C}{\partial y^2}=0, \tag{5.2.13}$$

Now, continuity equation is

$$\frac{\partial u}{\partial x}+\frac{\partial v}{\partial y}=0, \tag{5.2.14}$$

Momentum equation is

$$u\frac{\partial u}{\partial x}+v\frac{\partial u}{\partial y}-U_e\frac{dU_e}{dx}-\frac{1}{\rho}\frac{\partial}{\partial y}\left(\mu^*(T)\frac{\partial u}{\partial y}\right)-3\frac{\mu^*(T)}{\rho}\left(\frac{p_i-1}{2}\right)\Gamma^2\left(\frac{\partial u}{\partial y}\right)^2\frac{\partial^2 u}{\partial y^2}$$
$$-\frac{1}{\rho}\left(\frac{p_i-1}{2}\right)\Gamma^2\frac{\partial\mu^*(T)}{\partial y}\left(\frac{\partial u}{\partial y}\right)^3-\frac{\sigma\mathcal{B}^2}{\rho}\left(U_e-u\right)=0, \tag{5.2.15}$$

Energy equation is

$$u\frac{\partial T}{\partial x}+v\frac{\partial T}{\partial y}+\frac{1}{\rho C_p}\frac{\partial q_r}{\partial y}-\frac{\kappa}{\rho C_p}\frac{\partial^2 T}{\partial y^2}-\frac{D_M K_T}{C_p C_s}\frac{\partial^2 C}{\partial y^2}=0, \tag{5.2.16}$$

Concentration equation is

$$u\frac{\partial C}{\partial x}+v\frac{\partial C}{\partial y}-\frac{D_M K_T}{T_m}\frac{\partial^2 T}{\partial y^2}-D_M\frac{\partial^2 C}{\partial y^2}=0, \tag{5.2.17}$$

to the boundary conditions

$$\left.\begin{aligned} u=U_w\left(x\right),\ v=\ v_w\left(x\right),\ \ C=C_w,\ \frac{\partial T}{\partial y}=-\frac{q_0}{\kappa}x^{\frac{m-1}{2}},\ \text{at } y=0,\\ u=U_e\left(x\right),\ \ C\to C_\infty,\ \ T\to T_\infty,\ \text{as } y\to\infty. \end{aligned}\right\} \tag{5.2.18}$$

Heat flux by Rosseland [126] is:

$$q_r=-\frac{4\sigma^*\partial T^4}{3k^*\partial y} \tag{5.2.19}$$

Adegbie et al. [112] provide a mathematical model of temperature dependent viscosity

$$\mu\left(T\right)=\mu^*\left[1+h_1\left(T_\infty-T\right)\right], \tag{5.2.20}$$

where, h_1 is constant and its value depends on the fluid.
The introduction of similarity transformations

$$\left.\begin{aligned} u=b^*x^m f'\left(\eta\right),\ \ v=-\sqrt{b^*\nu}x^{\frac{m-1}{2}}\left[\left(\frac{m-1}{2}\right)\eta f'\left(\eta\right)+\left(\frac{m+1}{2}\right)f\left(\eta\right)\right],\\ \eta=\sqrt{\frac{b^*}{\nu}}yx^{\frac{m-1}{2}},\ \ \phi\left(\eta\right)=\frac{C-C_\infty}{C_w-C_\infty},\ \ \theta\left(\eta\right)=\sqrt{\frac{b^*}{\nu}}\frac{\kappa}{q_0}(T-T_\infty), \end{aligned}\right\} \tag{5.2.21}$$

Inserting Eq. (5.2.21) in Eqs. (5.2.14)-(5.2.17) and (5.2.18), Equation (5.2.14) is

identically satisfied and Eqs. (5.2.15)-(5.2.17) and (5.2.18) will be

$$(1-\zeta\theta)\left[1+3\left(\frac{p_i-1}{2}\right)We^2f''f''\right]f'''-m(f'f'-1)-M^2(f'-1)$$
$$-\zeta\left[1+\left(\frac{p_i-1}{2}\right)We^2f''f''\right]f''\theta'+\left(\frac{1+m}{2}\right)ff''=0, \quad (5.2.22)$$

$$\left(1+\frac{4}{3}Rd\left\{(\theta_w-1)\,\theta+1\right\}^3\right)\theta''+DuPr\phi''+4Rd\left((\theta_w-1)\,\theta+1\right)^2(\theta_w-1)\,\theta'\theta'$$
$$+Pr\left(\frac{m+1}{2}\right)\theta'f=0, \quad (5.2.23)$$

$$\phi''+\frac{m+1}{2}Scf\phi'+ScSr\theta''=0, \quad (5.2.24)$$

$$f(\eta)=f_w,\ f'(\eta)=B,\ \theta'(\eta)=-1,\ \phi(\eta)=1,\ \text{ at }\ \eta=0, \quad (5.2.25)$$
$$f'(\eta)=1,\ \theta(\eta)=\ \phi(\eta)=0.\ \text{ as }\ \eta\to\infty. \quad (5.2.26)$$

Skin friction coefficient C_{fx}, Nusselt count Nu_x and Sherwood count Sh_x are the physical measures of concern in this study, and they are described as,

$$C_{fx}=\tau_w(x)\,\rho U_e^2, \quad (5.2.27)$$

$$\text{where, surface shear stress } \tau_w(x)=\mu(T)\left\{1+3\Gamma^2\left(\frac{p_i-1}{2}\right)\left(\frac{\partial u}{\partial y}\right)^2\right\}\left.\frac{\partial u}{\partial y}\right|_{y=0}, \quad (5.2.28)$$

$$\text{then }\ C_fRe_x^{\frac{1}{2}}=(1-\zeta\theta(0))\left[1+3\left(\frac{p_i-1}{2}\right)We^2f''(0)\,f''(0)\right]f''(0), \quad (5.2.29)$$

$$Nu_x=\frac{xq_w(x)}{\kappa(T-T_\infty)}, \quad (5.2.30)$$

$$\text{where, surface heat flux } q_w(x)=\left(-\kappa\frac{\partial T}{\partial y}+q_r\right)_{y=0} \quad (5.2.31)$$

$$\text{then } Nu_xRe_x^{-\frac{1}{2}}=\frac{\left(1+\frac{4}{3}Rd\left\{(\theta_w-1)\,\theta(0)+1\right\}^3\right)}{\theta(0)}, \quad (5.2.32)$$

$$Sh_x=\frac{xq_m}{D_M(C_w-C_\infty)},\ \text{where surface mass flux } q_m=-D_M\left.\frac{\partial C}{\partial y}\right|_{y=0}, \quad (5.2.33)$$

$$\text{then } Sh_xRe_x^{-\frac{1}{2}}=-\phi'(0), \quad (5.2.34)$$

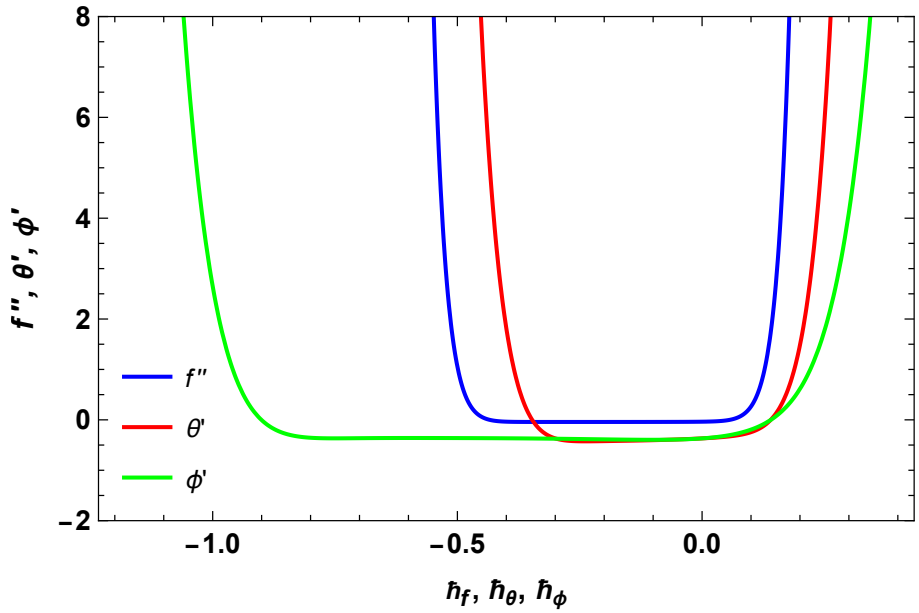

Figure 5.1: $\hbar$-curve for range f'', θ' and ϕ'.

where $Re_x^{\frac{1}{2}} = \sqrt{\frac{b^*}{\nu}} x^{\frac{m+1}{2}}$.

5.3 Solution by Homotopy Analysis Method

Liao [121] established HAM. Initial guesses and linear operators are described in that kind of a manner that they gratify the boundary conditions given in Eq. (5.2.18). Initial guesses

$$f_0(\eta) = \eta + (f_w + B - 1) + (1 - B)\, e^{-\eta}, \quad \theta_0(\eta) = e^{-\eta}, \quad \phi_0(\eta) = e^{-\eta}, \tag{5.3.1}$$

and linear operators

$$\mathcal{L}_f = \frac{\partial^3 f}{\partial \eta^3} + \frac{\partial^2 f}{\partial \eta^2}, \quad \mathcal{L}_\theta = \frac{\partial^2 \theta}{\partial \eta^2} + \frac{\partial \theta}{\partial \eta}, \quad \mathcal{L}_\phi = \frac{\partial^2 \phi}{\partial \eta^2} + \frac{\partial \phi}{\partial \eta}, \tag{5.3.2}$$

Satisfying

$$\mathcal{L}_f\left(k_1 + k_2\eta + k_3 e^{-\eta}\right) = 0, \mathcal{L}_\theta\left(k_4 + k_5 e^{-\eta}\right) = 0, \mathcal{L}_\phi\left(k_6 + k_7 e^{-\eta}\right) = 0. \tag{5.3.3}$$

where arbitrary constants are k_i, $(i = 1,\ 2, \ldots, 7)$.

5.4 Convergence Analysis

For the appropriate choice of $\hbar_f$, $\hbar_\theta$ and $\hbar_\phi$ HAM solutions converges. $f''(1)$, $\theta'(1)$ and $\phi'(1)$ are plotted upto the suitable approximations. We can choose $\hbar_f = -0.4$, $\hbar_\theta = -0.5$ and $\hbar_\phi = -1.0$ from Figure 5.1.

5.5 Conclusion

The main findings of the research are following:

- Velocity field increases for variable viscosity parameter, Nonlinear parameter and Suction parameter for shrinking and stretching cases.
- For large amount of Magnetic parameter and Weissenberg number velocity field increases in shrinking case and behaves opposite in stretching case.
- For large value of power index, velocity decreases in shrinking case and reverse effect ouccurs for stretching case.
- Temperature enhances for large amount of Magnetic parameter, Temperature ratio parameter, Dufour number and Radiation parameter, and gives reverse impact for nonlinear parameter.
- Concentration field increases for Soret number and behaves opposite for Schimdt number.
- Skin friction coefficient increases with increaseing values of Suction parameter for shrinking case and decreasing for stretching case.
- Nusselt count increases for large amount of temperature ratio parameter.
- For increasing values of Soret number, Sherwood count increases.

Chapter 6

Unsteady MHD flow of a Micropolar fluid over a stretching sheet

Unsteady flow is used in a variety of devices, including reciprocating engines, pressure exchangers, hydraulic rams, and ocean wave machines. Design of chemical processing equipment, fog formation and dispersion, temperature and moisture distribution over agricultural fields and orchards of fruit trees, crop damage from freezing, food processing, and cooling towers are a few representative fields of interest where combined heat and mass transfer with chemical reaction effect plays an important role.

6.1 Novelty of the Chapter

In this Chapter,the impact of nonlinear radiation on the mixed convection flow of unsteady Micropolar fluid over an stretching sheet considering chemical reaction. The solution to the problem encountered by using the method of Homotopy analysis

6.2 Mathematical Formulation of the Problem

Consider an unsteady two-dimensional MHD flow of an incompressible Micropolar fluid, heat and mass transfer over a vertical stretching sheet. The sheet is assumed to emerge vertically in the upward direction from a narrow slot with velocity

$$U_w\left(x,\ t\right) = \frac{ax}{1-\alpha t}, \tag{6.2.1}$$

where both a and α are positive constants with dimension per unit time. We measure the positive x direction along the stretching sheet with the slot as the origin. We then measure the positive y coordinate perpendicular to the sheet in the outward direction toward the fluid flow. The surface temperature T_w and concentration C_w

of the stretching sheet vary with the distance x from the sheet and time t as

$$T_w\left(x,\ t\right) = T_\infty + \ \frac{bx}{\left(1-\alpha t\right)^2}, \quad C_w\left(x,\ t\right) = C_\infty + \ \frac{cx}{\left(1-\alpha t\right)^2}, \tag{6.2.2}$$

where b, c are constants with dimension of temperature and concentration, respectively, over length. It is noted that the expressions for $U_w(x,t)$, $T_w(x,t)$, and $C_w(x,t)$ are valid only for $t < \alpha^{-1}$. We also remark that the sheet which is fixed at the origin is stretched by applying a force in the x-direction and the effective stretching rate $a/(1-\alpha t)$ increases with time. The sheet temperature and concentration increase (reduce) if b and c are positive (negative), respectively. We assume that the radiation effect is significant in this study. The fluid properties are taken to be constant except for density variation with temperature and concentration in the buoyancy terms. Under those assumptions and the Boussinesq approximations, the governing boundary layer equations are given as:

$$\frac{\partial u}{\partial x} + \frac{\partial v}{\partial y} = 0, \tag{6.2.3}$$

$$\frac{\partial u}{\partial t} + u\frac{\partial u}{\partial x} + v\frac{\partial u}{\partial y} = \left(\frac{\mu + k}{\rho}\right)\frac{\partial^2 u}{\partial y^2} + \frac{k}{\rho}\frac{\partial G}{\partial y} + g\beta_T\left(T - T_\infty\right) + g\beta_C\left(C - C_\infty\right) - \frac{\sigma \mathcal{B}^2 u}{\rho}, \tag{6.2.4}$$

$$\frac{\partial G}{\partial t} + u\frac{\partial G}{\partial x} + v\frac{\partial G}{\partial y} = \frac{\gamma^*}{\rho j}\frac{\partial^2 G}{\partial y^2} - \frac{k}{\rho j}\left(2G + \frac{\partial u}{\partial y}\right), \tag{6.2.5}$$

$$\frac{\partial T}{\partial t} + u\frac{\partial T}{\partial x} + v\frac{\partial T}{\partial y} = \kappa\left(\frac{\partial^2 T}{\partial y^2}\right) - \frac{1}{\rho C_P}\frac{\partial q_r}{\partial y} + \left(\frac{\mu + k}{\rho}\right)\left(\frac{\partial u}{\partial y}\right)^2, \tag{6.2.6}$$

$$\frac{\partial C}{\partial t} + u\frac{\partial C}{\partial x} + v\frac{\partial C}{\partial y} = D_M\frac{\partial^2 C}{\partial y^2} + k_c\left(C - C_\infty\right), \tag{6.2.7}$$

with the appropriate boundary conditions

$$u = U_w\left(x,\ t\right), \quad v = 0, \quad G = 0, \quad T = T_w\left(x,\ t\right), \quad C = C_w\left(x,\ t\right) \quad \text{at} \quad y = 0, \tag{6.2.8}$$

$$u \to 0, \quad G \to 0, \quad T \to T_\infty, \quad C \to C_\infty \quad as \to \infty. \tag{6.2.9}$$

Radiative heat flux q_r is given by Rosseland [126]

$$q_r = \frac{4}{3}\frac{\sigma^*}{k^*}\frac{\partial T^4}{\partial y}, \tag{6.2.10}$$

We recommend similarity variables reconstruct the governing equations (6.2.3)-(6.2.9) into the system of ordinary differential equations,

$$\eta = \sqrt{\frac{a}{\nu\left(1-\alpha t\right)}}y, \quad u = \ \frac{ax}{1-\alpha t}f'\left(n\right), \quad v = -\sqrt{\frac{a}{v\left(1-\alpha t\right)}}f\left(\eta\right), \tag{6.2.11}$$

$$G=\sqrt{\frac{a^3}{v\left(1-\alpha t\right)^3}}xh\left(\eta\right),\quad T=T_\infty+\frac{bx}{\left(1-\alpha t\right)^2}\theta\left(\eta\right),\quad C=C_\infty+\frac{cx}{\left(1-\alpha t\right)^2}\phi\left(\eta\right), \tag{6.2.12}$$

We get

$$\left(1+K\right)f'''+ff''-f'^2-\frac{A}{2}\left(2f'+\eta f''\right)+Kh'+Gr_T\theta+Gr_C\phi-M^2f'=0, \tag{6.2.13}$$

$$\lambda 3h''+fh'-f'h-\frac{A}{2}\left(3h+\eta h'\right)-K\lambda_4\left(2h+f''\right)=0, \tag{6.2.14}$$

$$\left(1+\frac{4}{3}Rd\left(\left(\theta_w-1\right)\theta+1\right)^3\right)\theta''+4Rd\left(\left(\theta_w-1\right)\theta+1\right)^2\left(\theta_w-1\right)\theta'^2+Prf\theta'$$
$$-Prf'\theta-\frac{A}{2}Pr\left(4\theta+\eta\theta'\right)+PrEc\left(1+K\right)f''^2=0, \tag{6.2.15}$$

$$\frac{1}{Sc}\phi''+f\phi'-f'\phi-K_c\phi-\frac{A}{2}\left(4\phi+\eta\phi'\right)=0, \tag{6.2.16}$$

with

$$f\left(0\right)=0,\quad f'\left(0\right)=1,\quad h\left(0\right)=0,\ \theta\left(0\right)=1,\quad \phi\left(0\right)=1, \tag{6.2.17}$$
$$f'\left(\infty\right)=0,\quad h\left(\infty\right)=0,\quad \theta\left(\infty\right)=0,\quad \phi\left(\infty\right)=0, \tag{6.2.18}$$

where $A=\dfrac{\alpha}{a}$, $K=\dfrac{\kappa}{\mu}$, $Gr_T=\dfrac{g\beta_t b}{a^2}$, $Gr_C=\dfrac{g\beta_c c}{a^2}$, $\lambda_3=\dfrac{\gamma^*}{\mu j}$, $\lambda_4=\dfrac{\nu\left(1-\alpha t\right)}{aj}$, $Ec=\dfrac{U_w^2}{C_p\left(T_w-T_\infty\right)}$, $Sc=\dfrac{\nu}{D_M}$, $Rd=\dfrac{4\sigma^*T_\infty^3}{k^*\kappa}$, $\theta_w=\dfrac{T_w}{T_\infty}$.

Skin friction coefficient, wall couple stress, Nusselt number and Sherwood number in dimension form are given as

$$\begin{aligned}&C_{fx}=\frac{2}{\rho U_w^2}\left[\left(\mu+k\right)\frac{\partial u}{\partial y}+kG\right]_{y=0},\ M_{wx}=\frac{\gamma^*a}{\nu}\left(\frac{\partial G}{\partial y}\right)_{y=0},\\&Nu_x=\frac{-x}{T_w-T_\infty}\left(1+\frac{16\sigma^*T^3}{3k^*\kappa}\right)\frac{\partial T}{\partial y}_{y=0},\ Sh_x=\frac{-x}{C_w-C_\infty}\left(\frac{\partial C}{\partial y}\right)_{y=0}.\end{aligned} \tag{6.2.19}$$

Physical measures are given by

$$\begin{aligned}Re_x^{\frac{1}{2}}Cf_x=2\left(1+K\right)f''\left(0\right),\quad Re_x^1M_{wx}=h'\left(0\right),\quad Re_x^{-1/2}Sh_x=-\phi'\left(0\right),\\Re_x^{-1/2}Nu_x=-\left(1+\frac{4}{3}Rd\left\{1+\left(\theta_w-1\right)\theta\left(0\right)\right\}^3\right)\theta'\left(0\right),\end{aligned} \tag{6.2.20}$$

6.3 Solution by Homotopy Analysis Method

There is also great flexibility concerning the Homotopy analysis approach to select the initial suppositions and the auxiliary linear operators $f_0\left(\eta\right)$, $h_0\left(\eta\right)$, $\theta_0\left(\eta\right)$ and

$\phi_0(\eta)$ and linear operators $\mathcal{L}_f$, $\mathcal{L}_h$, $\mathcal{L}_\theta$ and $\mathcal{L}_\phi$ are so taken as to satisfy boundary conditions of the given in equations (6.2.8)-(6.2.9).
Initial guesses are

$$f_0(\eta) = 1 - e^{-\eta}, \quad h_0(\eta) = 0, \quad \theta_0(\eta) = e^{-\eta}, \quad \phi_0(\eta) = e^{-\eta}, \tag{6.3.1}$$

with auxiliary linear operators

$$\mathcal{L}_f = \frac{\partial^3 f}{\partial \eta^3} - \frac{\partial f}{\partial \eta}, \quad \mathcal{L}_h = \frac{\partial^2 h}{\partial \eta^2} - h, \quad \mathcal{L}_\theta = \frac{\partial^2 \theta}{\partial \eta^2} - \theta, \quad \mathcal{L}_\phi = \frac{\partial^2 \phi}{\partial \eta^2} - \phi, \tag{6.3.2}$$

satisfying

$$\mathcal{L}_f\left(k_1 + k_2 e^{\eta} + k_3 e^{-\eta}\right) = 0, \ \mathcal{L}_h\left(k_4 e^{\eta} + k_5 e^{-\eta}\right) = 0, \tag{6.3.3}$$

$$\mathcal{L}_\theta\left(k_6 e^{\eta} + k_7 e^{-\eta}\right) = 0, \ \mathcal{L}_\phi\left(k_8 e^{\eta} + k_9 e^{-\eta}\right) = 0, \tag{6.3.4}$$

6.3.1 Convergence Analysis

Their HAM solutions converge significantly with the parameter values $\hbar_f$, $\hbar_h$, $\hbar_\theta$ and $\hbar_\phi$. The necessary curves are shown in the plots for this purpose. In this case, a HAM approximation is used to draw $\hbar$-curves. Figures 6.1 - **??** imply range: $-1.6 \leq \hbar_f \leq -0.4$ for the auxiliary parameter $\hbar_f$, $-3.2 \leq \hbar_h \leq -0.5$ for the auxiliary parameter $\hbar_h$, $-1.5 \leq \hbar_\theta \leq -0.5$ for the auxiliary parameter $\hbar_\theta$ and $-0.35 \leq \hbar_\phi \leq -0.1$ for the auxiliary parameter $\hbar_\phi$ respectively.

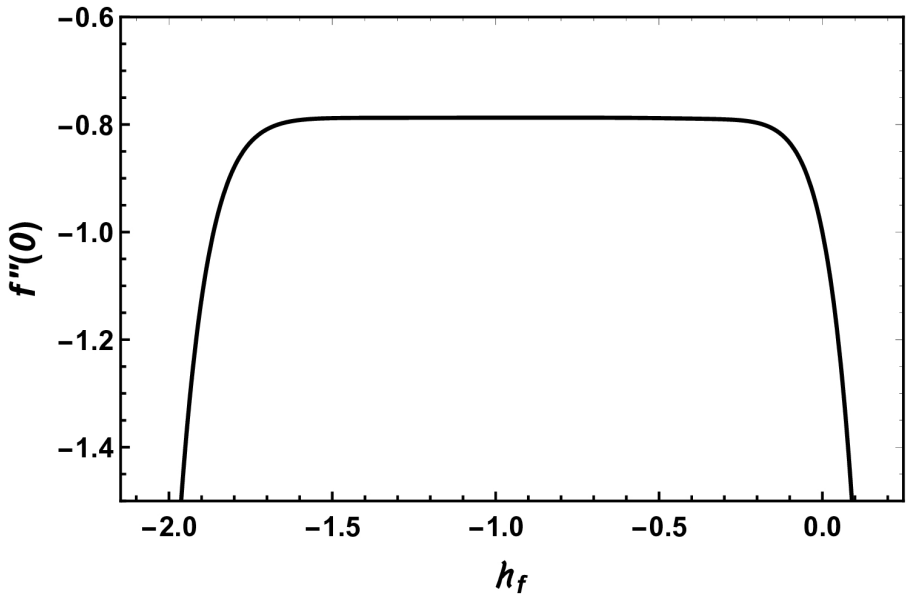

Figure 6.1: $f''(0)$ via $\hbar_f$

6.4 Conclusion

This paper examines the effects of non-linear radiation on MHD mixed convection flow of Micropolar fluid over unsteady stretching sheet accurately. By applying the

method of Homotopy analysis, the dimensionless governing equations are solved. By drawing the so-called $\hbar$ -curve the convergence region of series solutions by HAM is achieved. We thought of Micropolar fluid. The results for axial velocity, angular velocity, temperature, and concentration are obtained and are graphical. The key results of this study are:

- Axial velocity profile of the Micropolar fluid declines for large values in Magnetic Parameter M and unsteadiness parameter A.
- Micropolar fluid axial velocity profile enhances for Eckert number Ec and Micropolar parameter K. The Micropolar fluid angular velocity profile enhances for broad values of Micropolar parameter K, λ_4 and declines with high values of unsteadiness parameter A and thermal Grashof number Gr_T.
- The temperature profile of the Micropolar fluid declines for high values Micropolar parameter K and Temperature ratio θ_w.
- The temperature of the object changes as it's subjected to a great magnetic field and exposure to radiation.
- For the large values of unsteadiness parameter A, thermal Grashof number Gr_T and Schmidt number Sc decreases concentration profile of the Micropolar fluid.
- For large values of Magnetic parameter M, concentration profile increases.
- Skin friction, Wall couple stress and decreases for the broad unsteadiness parameter A values.
- Nusselt number increases with large amount of Prandtl number Pr.

Chapter 7

Entropy optimized unsteady MHD Williamson fluid flow considering viscous dissipation effects

Viscous dissipation is of importance for a variety of applications; for instance, large temperature increases are seen during high-speed polymer manufacturing operations like injection moulding or extrusion. The thin boundary layer surrounding fast aircraft experiences aerodynamic heating, which boosts skin temperature. Due to numerous applications of convective boundary conditions in technology, including thermal energy storage, petroleum processing, material drying etc, we considered convective boundary conditions in this chapter.

7.1 Novelty of the Chapter

In light of the above studies, the aim of this investigation is to analyze joule heating, nonlinear radiation and viscous dissipation effects on unsteady Natural convective flow of MHD williamson fluid across a stretching sheet. Convective boundary conditions, slip effect and entropy generation rate are included in this investigation.

7.2 Mathematical Formulation of the Problem

It is assumed that two dimensional, unsteady flow of an incompressible Williamson fluid across a stretching sheet with joule heating, nonlinear radiation and viscous dissipation have been considered. Entropy generation rate is discussed here. The slip condition and convective boundary conditions have been addressed. As seen in Figure 7.1 the vertical axis was chosen transverse to the surface, and we decided to use the cartesian system to measure the sheet along the x, y, and x axes that were chosen next to the stretching sheet. Non-uniform velocity of the sheet is $U_w(x,t) = \frac{bx}{1-\alpha t}$, where b is the rate of stretching sheet with respect to x axis where αt is a positive constant according to case $\alpha t < 1$. Where $\mathcal{B} = B_0/\sqrt{1-\alpha t}$ is the magnetic

field's strength and is applied in the direction of the positive y axis, Comparing the magnetic Reynolds number to the induced magnetic field, it is very small.

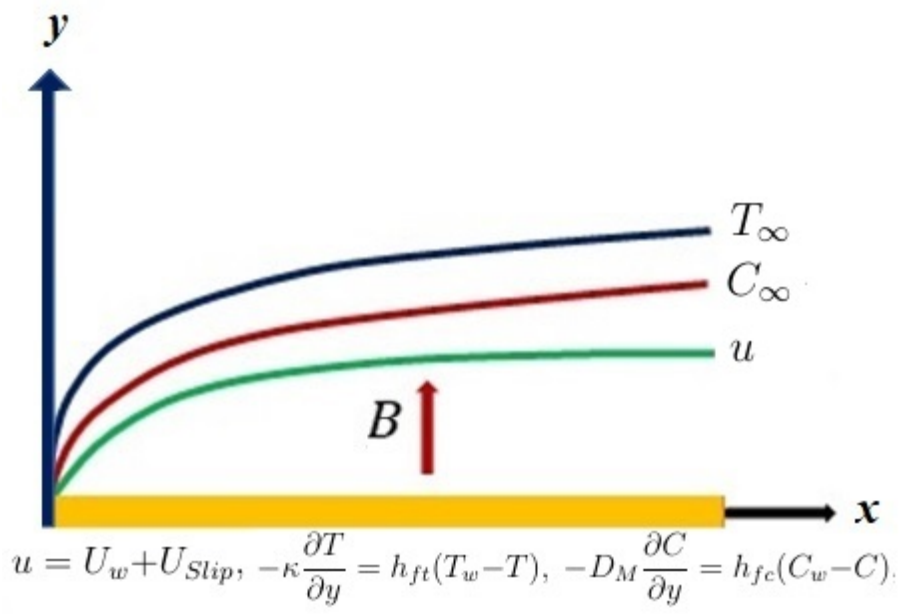

Figure 7.1: Physical Sketch of the Problem

Governing equations for Williamson fluid are as follows:

$$\frac{\partial u}{\partial x} + \frac{\partial v}{\partial y} = 0, \tag{7.2.1}$$

$$\frac{\partial u}{\partial t} + u\frac{\partial u}{\partial x} + v\frac{\partial u}{\partial y} = \nu\frac{\partial^2 u}{\partial y^2} + \sqrt{2}\Gamma\nu\frac{\partial^2 u}{\partial y^2}\frac{\partial u}{\partial y} - \frac{\sigma B^2}{\rho}u + g\beta_C(C - C_\infty) + g\beta_T(T - T_\infty), \tag{7.2.2}$$

$$\frac{\partial T}{\partial t} + u\frac{\partial T}{\partial x} + v\frac{\partial T}{\partial y} = \frac{\kappa}{\rho C_p}\frac{\partial^2 T}{\partial y^2} - \frac{1}{\rho C_p}\frac{\partial q_r}{\partial y} + \frac{\sigma\mathcal{B}^2}{\rho C_p}u^2 + \frac{\mu}{\rho C_p}\left(\frac{\partial u}{\partial y}\right)^2, \tag{7.2.3}$$

$$\frac{\partial C}{\partial t} + u\frac{\partial C}{\partial x} + v\frac{\partial C}{\partial y} = D_M\frac{\partial^2 C}{\partial y^2} + k_c(C - C_\infty), \tag{7.2.4}$$

where u is the velocity components along the x-axis and v with the y-axis, respectively. β_T, β_C, g and Γ are thermal expansion coefficient, concentration expansion coefficient, gravity and time fluid parameter respectively. T_w and C_w symbolizes surface temperature and concentration, respectively. D_M and k_c are mass diffusivity and reaction rate constant. Linearized Heat flux by Rosseland [126] is:

$$q_r = -\frac{16\sigma^* T_\infty^3}{3k^*}\frac{\partial T}{\partial y}, \tag{7.2.5}$$

where k^* and σ^* are mean absorption coefficient and Stefan-Boltzmann constant respectively. In light of the necessity of nonlinear lradiation, we convert T_∞^3 with T^3

in Equation (7.2.6), then

$$q_r = -\frac{16\sigma^* T^3}{3k^*}\frac{\partial T}{\partial y}, \tag{7.2.6}$$

The mathematical model has the following boundary conditions

$$u = U_w + U_{Slip}, \quad v = v_w = \frac{v_0}{\sqrt{1-\alpha t}}, \; -\kappa\frac{\partial T}{\partial y} = h_{ft}(T_w - T),$$
$$-D_M\frac{\partial C}{\partial y} = h_{fc}(C_w - C), \quad at \quad y = 0, \tag{7.2.7}$$

$$u \to 0, \quad T \to T_\infty, C \to C_\infty, \; at \quad y \to \infty. \tag{7.2.8}$$

Introducing the following transformation to convert equations (7.2.1)-(7.2.4) and equation (7.2.7)-(7.2.8) into nonlinear ordinary differential equations,

$$\eta = \sqrt{\frac{b}{\nu(1-\alpha t)}}y, \quad u = \frac{bx}{(1-\alpha t)}f'(\eta), \quad v = -\sqrt{\frac{b\nu}{1-\alpha t}}f(\eta),$$
$$B = \frac{B_0}{\sqrt{1-\alpha t}}, \; T_w = T_\infty + \frac{b^* x}{(1-\alpha t)^2}, \; C_w = C_\infty + \frac{c^* x}{(1-\alpha t)^2},$$
$$T = T_\infty + \frac{b^* x}{(1-\alpha t)^2}\theta(\eta), \quad C = C_\infty + \frac{c^* x}{(1-\alpha t)^2}\phi(\eta), \tag{7.2.9}$$

Using the similarity variables above Equation (7.2.1) is fulfilled. Equations (7.2.2)-(7.2.4) and (7.2.7)-(7.2.8) will be converted into the following nonlinear ordinary differential equations:

$$f'''(1 + Wef'') + ff'' - Mf' + Gr_T\theta + Gr_C\phi - f'f' - A\left[f' + \left(\frac{\eta}{2}\right)f''\right] = 0, \tag{7.2.10}$$

$$\left(1 + \frac{4}{3}Rd\left\{1 + (\theta_w - 1)\theta\right\}^3\right)\theta'' + 4Rd\left\{1 + (\theta_w - 1)\theta\right\}^2(\theta_w - 1)\theta'^2$$
$$+ Pr\left[Ecf''^2 + EcMf'^2 - f'\theta + f\theta' - 2A\left\{\theta + \left(\frac{\eta}{4}\right)\theta'\right\}\right] = 0, \tag{7.2.11}$$

$$\phi'' + Sc\left[\phi' f - f'\phi - K_c\phi - 2A\left\{\phi + \left(\frac{\eta}{4}\right)\phi'\right\}\right] = 0, \tag{7.2.12}$$

with

$$f(0) = f_w, \quad f'(0) = 1 + \gamma f''(0), \quad \theta'(0) = \lambda_1(\theta(0) - 1),$$
$$\phi'(0) = \lambda_2(\phi(0) - 1), \theta(\infty) = \quad f'(\infty) = \quad \phi(\infty) = 0. \tag{7.2.13}$$

where $We = \sqrt{\frac{2\Gamma^2 b^3 x^2}{\nu(1-\alpha t)^3}}$, $Pr = \frac{\mu C_p}{\kappa}$, $M = \frac{\sigma B_0^2}{\rho b}$, $\theta_w = \frac{T_w}{T_\infty}$, $Rd = \frac{4\sigma^* T_\infty^3}{k^*\kappa}$, $Gr_T = \frac{gb^*\beta_T}{b^2}$, $Sc = \frac{\nu}{D_M}$, $Gr_C = \frac{gc^*\beta_C}{b^2}$, $A = \frac{\alpha}{b}$, $Ec = \frac{b^2 x}{b^* C_p}$, $f_w = -\frac{v_0}{\sqrt{b\nu}}$, $K_c = \frac{k_c}{b}$,

$\gamma = \alpha\mu\sqrt{\dfrac{b}{\nu(1-\alpha t)}}$, $\lambda_1 = -\dfrac{h_{ft}}{\kappa}\sqrt{\dfrac{\nu(1-\alpha t)}{b}}$ and $\lambda_2 = -\dfrac{h_{fc}}{D_M}\sqrt{\dfrac{\nu(1-\alpha t)}{b}}$.

Skin friction coefficient, rate of heat and mass transfer at the wall are respectively,

$$C_f = \frac{\tau_w}{\rho U_w^2}, Nu = \frac{xq_w}{\kappa(T_w - T_\infty)}, Sh = \frac{xq_m}{D_M(C_w - C_\infty)} \tag{7.2.14}$$

At the wall, τ_w, q_m and q_w denote shear stress, mass and heat diffusion respectively, where τ_w, q_m and q_w defined as:

$$\tau_w = \mu\left[\frac{\partial u}{\partial y} + \Gamma\left(\frac{\partial u}{\partial y}\right)^2\right]_{y=0}, q_w = -\kappa\left(1 + \frac{16\sigma^* T^3}{3\kappa k^*}\right)\left.\frac{\partial T}{\partial y}\right|_{y=0}, q_m = -D_M\left.\frac{\partial C}{\partial y}\right|_{y=0}, \tag{7.2.15}$$

using similarity variables, Skin friction factor, Nusselt and Sherwood numbers

$$C_f\left(Re_x^{1/2}\right) = f''(0) + We\left(f''(0)\right)^2, \quad ShRe_x^{-1/2} = -\phi'(0),$$
$$NuRe_x^{-1/2} = -\left(1 + \frac{4}{3}Rd\left\{1 + (\theta_w - 1)\theta(0)\right\}^3\right)\theta'(0), \tag{7.2.16}$$

where $Re_x = \dfrac{bx^2}{\nu(1-\alpha t)}$ is local Reynolds number.

Generation of entropy is

$$S_G = \underbrace{\frac{\kappa}{T_\infty^2}\left(1 + \frac{16\sigma^* T^3}{3\kappa k^*}\right)\left(\frac{\partial T}{\partial y}\right)^2}_{\text{heat transfer irreversibilty}} + \underbrace{\frac{\mu}{T_\infty}\left(\frac{\partial u}{\partial y}\right)^2}_{\substack{\text{viscous dissipation}\\ \text{irreversibilty}}} + \underbrace{\frac{\sigma B_0^2}{T_\infty}u^2}_{\substack{\text{Joule heating}\\ \text{irreversibilty}}} + \underbrace{\frac{RD}{C_\infty}\left(\frac{\partial C}{\partial y}\right)^2}_{\substack{\text{mass transfer}\\ \text{irreversibilty}}} \tag{7.2.17}$$

Applying similarity variables, we get

$$N_G = \alpha_1\left(1 + \frac{4}{3}Rd\left\{1 + (\theta_w - 1)\theta\right\}^3\right)\theta'^2 + Brf''^2 + MBrf'^2 + \left(\frac{L^*}{\alpha_1}\right)\alpha_2\phi'^2, \tag{7.2.18}$$

$$\text{Bejan number} Be = \frac{\text{Entropy generation due to heat and mass transfer}}{\text{Total entropy generation}} \tag{7.2.19}$$

then,

$$Be = \frac{\alpha_1\left(1 + \frac{4}{3}Rd\left\{1 + (\theta_w - 1)\theta\right\}^3\right)\theta'^2 + \left(\frac{L^*}{\alpha_1}\right)\alpha_2\phi'^2}{\alpha_1\left(1 + \frac{4}{3}Rd\left\{1 + (\theta_w - 1)\theta\right\}^3\right)\theta'^2 + Brf''^2 + MBrf'^2 + \left(\frac{L^*}{\alpha_1}\right)\alpha_2\phi'^2} \tag{7.2.20}$$

where $N_G = \dfrac{T_\infty\nu(1-\alpha t)}{b\kappa\left(T_w - T_\infty\right)}S_G$, $\alpha_1 = \dfrac{T_w - T_\infty}{T_\infty}$, $L^* = \dfrac{RDC_\infty}{\kappa}$, $\alpha_2 = \left(\dfrac{C_w - C_\infty}{C_\infty}\right)^2$.

7.3 Solution by Homotopy Analysis Method

Initial guesses and auxiliary linear operators respectively are

$$f_0(\eta) = f_w + \frac{1}{1+\gamma}\left[1 - e^{-\eta}\right], \quad \theta_0(\eta) = \frac{\lambda_1}{1+\lambda_1}e^{-\eta}, \quad \phi_0(\eta) = \frac{\lambda_2}{1+\lambda_2}e^{-\eta}, \tag{7.3.1}$$

$$\mathcal{L}_f = \frac{\partial^3 f}{\partial \eta^3} - \frac{\partial f}{\partial \eta}, \quad \mathcal{L}_\theta = \frac{\partial^2 \theta}{\partial \eta^2} - \theta, \quad \mathcal{L}_\phi = \frac{\partial^2 \phi}{\partial \eta^2} - \phi, \tag{7.3.2}$$

where $\mathcal{L}_f\left(k_1 + k_2 e^{\eta} + k_3 e^{-\eta}\right) = 0$, $\mathcal{L}_\theta\left(k_4 + k_5 e^{-\eta}\right) = 0$, $\mathcal{L}_\phi\left(k_6 + k_7 e^{-\eta}\right) = 0$, and $k_1, k_2, \ldots, k_7$ are arbitrary constants.

7.3.1 Convergence Analysis

It is vital to make sure that our series solution converges while using the HAM approach. The value of the auxiliary parameter $\hbar$ has a massive effect on the HAM solution's approximation convergence rate. We have a lot of flexibility in moniter-ing and modifying convergence zone of the series solution because to this auxiliary parameter. $f''(0)$, $\theta'(0)$ and $\phi'(0)$ are plotted at the 20^{th} order of approximations to find the acceptable values of $\hbar_f$, $\hbar_\theta$ and $\hbar_\phi$. The selection of the values for $\hbar_f$, $\hbar_\theta$ and $\hbar_\phi$ ensures that curves are collinear to the horizontal axis. The permissible range for values of $\hbar_f$ $(-1.1 < \hbar_f < -0.2)$, $\hbar_\theta$ $(-1.3 < \hbar_\theta < 0.1)$ and $\hbar_\phi$ $(-0.5 < \hbar_\phi < 0.0)$ is clearly seen in Figure 7.2. Based on the present computations, $\hbar_f = -0.85$, $\hbar_\theta = -0.94$ and $\hbar_\phi = -0.34$ are used. Table **??** is provided to guarantee the con-vergence of solutions. The convergence is attained at the 30^{th}- order of estimations, as this table clearly demonstrates.

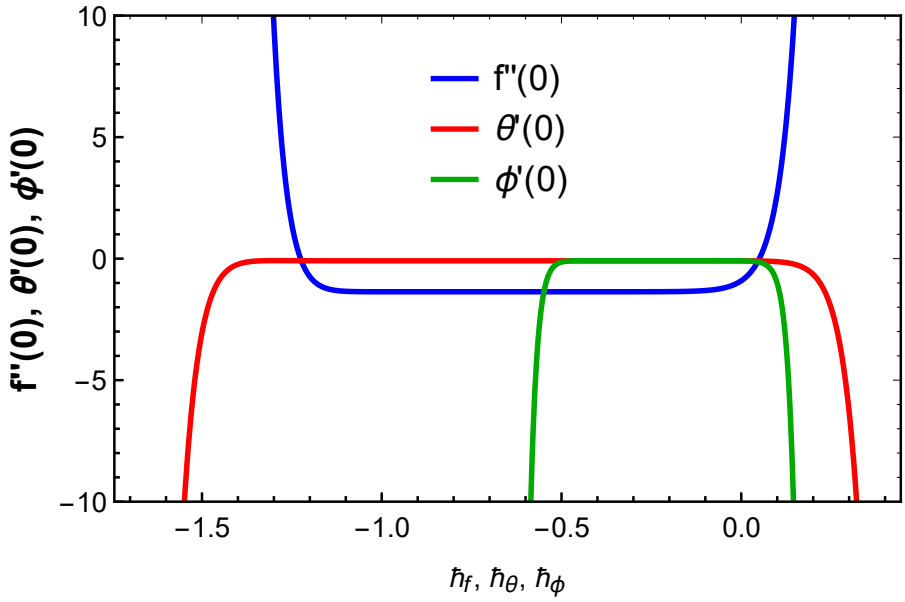

Figure 7.2: $f''(0)$ for $\hbar_f$

7.4 Conclusion

The intention of this research is to analyze joule heating, nonlinear radiation and viscous dissipation effects on entropy optimized unsteady Natural convective flow of MHD Williamson fluid across a stretching sheet with convective boundary conditions and slip condition . The main findings of the research are following:

- M, We and f_w reduces the flow.
- M, Rd, θ_w, Ec improves the temperature while Pr declines temperature.
- K_c and Sc increases concentration.
- A reduces the flow, temperature, and concentration distribution.
- N_G increases for L^*, Br and M.
- Be enhances for L^*, while declines for Br and M.
- C_{fx} improves for Gr_C and We.
- Nu_x declines for θ_w, whereas Sh_x enhances for K_c.

Chapter 8

EMHD fluid flow with slip effects

Electromagnetohydrodynamic (EMHD) is the area that concerns the study of dynamics of electrically conducting fluids under the influence of magnetic and electric fields. EMHD has raised quite an interest over the years due to its versatile application in geophysics, engineering, biomedical engineering, magnetic drug targeting, and many others. The non-adherence of the fluid to a solid boundary, known as velocity slip, occurs under certain circumstances. Fluids displaying slip are essential for technologies such as internal cavities and in the artificial cardiac valve polishing.

8.1 Novelty of the Problem

In this research, the aim of this investigation is to analyze EMHD flow of Micropolar fluid over a stretching sheet. The energy equation includes nonlinear thermal radiation and joule heating effects. Slip condition and convective boundary conditions are considered.

8.2 Mathematical Formulation of the Problem

Two dimensional incompressible Micropolar fluid flow through a horizontal sheet is considered. Figure 8.1 shows velocity of the stretching sheet is taken as $u = ax + U_{Slip}$. A magnetic fleld of strength $\mathcal{B}$ is normally applied with the conjecture of lower Reynolds number, so that the induced magnetic field may be ignored. Viscous dissipation and Joule heating and nonlinear thermal radiation effects are accounted. The surface of the stretching plate is in contact with another hot plate of temperature T_w and concentration C_w with h_{ft} and h_{fc} are the heat transfer coefficient and mass transfer coefficient. The volume of particle concentration and the temperature of the Micropolar fluid far away from the plate is supposed to be C_∞ and T_∞ respectively.

$$\frac{\partial u}{\partial x} + \frac{\partial v}{\partial y} = 0, \tag{8.2.1}$$

$$u\frac{\partial u}{\partial x} + v\frac{\partial u}{\partial y} = \left(\frac{\mu + k}{\rho}\right)\frac{\partial^2 u}{\partial y^2} + \frac{k}{\rho}\frac{\partial G}{\partial y} + \frac{\sigma}{\rho}\left(E_0 B_0 - B_0^2 u\right), \tag{8.2.2}$$

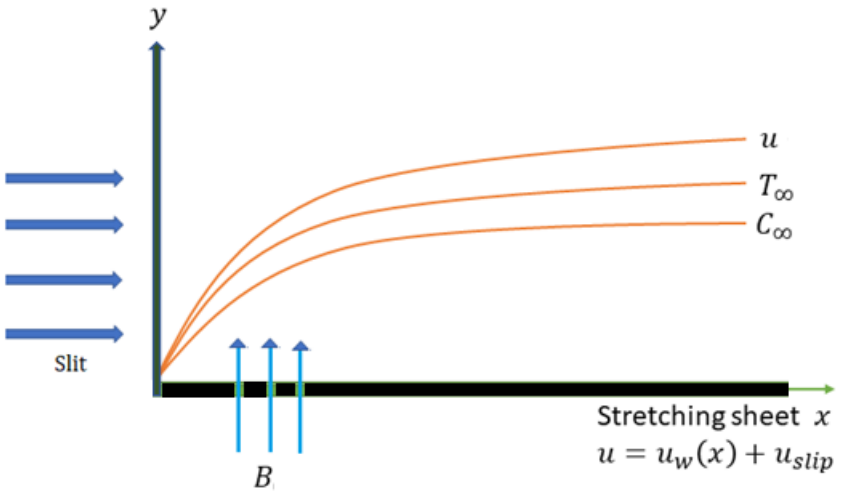

Figure 8.1: Physical Sketch of the Problem

$$u\frac{\partial G}{\partial x}+v\frac{\partial G}{\partial y}=\frac{\gamma^{*}}{\rho j}\frac{\partial^{2}G}{\partial y^{2}}-\frac{k}{\rho j}\left(2G+\frac{\partial u}{\partial y}\right), \tag{8.2.3}$$

$$u\frac{\partial T}{\partial x}+v\frac{\partial T}{\partial y}=\frac{\kappa}{\rho C_{P}}\left(\frac{\partial^{2}T}{\partial y^{2}}\right)+\frac{\left(uB_{0}-E_{0}\right)^{2}\sigma}{\rho C_{P}}-\frac{1}{\rho C_{P}}\frac{\partial q_{r}}{\partial y}+\left(\frac{\mu+k}{\rho}\right)\left(\frac{\partial u}{\partial y}\right)^{2}, \tag{8.2.4}$$

$$u\frac{\partial C}{\partial x}+v\frac{\partial C}{\partial y}=D_{M}\frac{\partial^{2}C}{\partial y^{2}}, \tag{8.2.5}$$

The variable formula can also be used here to identify these differential equations because it has a energy integral that is useful for the structure of the solution.

$$\begin{aligned}
&u=U_{w}\left(x\right)+U_{slip}=ax+\alpha^{*}\left[\left(\mu+k\right)\frac{\partial u}{\partial y}+kG\right],\ v=\ v_{w},G=-n\frac{\partial u}{\partial y},\\
&-\kappa\frac{\partial T}{\partial y}=h_{ft}\left(T_{f}-T\right),\ -D_{M}\frac{\partial C}{\partial y}=h_{fc}\left(C_{f}-C\right)\ \text{at}\ y=0,\\
&u\left(\infty\right)=G\left(\infty\right)=0,\ T\left(\infty\right)=T_{\infty},\ C\left(\infty\right)=C_{\infty}.
\end{aligned} \tag{8.2.6}$$

Heat flux is given by Rossland [126]:

$$q_{r}=-\frac{4\sigma^{*}}{3k^{*}}\frac{\partial T^{4}}{\partial y}, \tag{8.2.7}$$

where σ^{*} and k^{*} are Stephen Boltzmann's constant and coefficient of mean absorption respectively.

Instance $n=0,\ G=0$ on the surface is indicated. It shows a focused particle flow that cannot turn the micro-components nearest to the wall. This situation is often referred to as the high microelement concentration. Because the antisymmetric component of the stress tensor vanishes, the probability $n=0.5$ implies a low concentration of microelements. The turbulent boundary layer flows are modelled

using the case $n = 1$. Consider the following similarity transformation.

$$\left.\begin{aligned} u = axf'(\eta), v = -\sqrt{a\nu} f(\eta), \phi(\eta) = \frac{C - C_\infty}{C_w - C_\infty}, \theta(\eta) = \frac{T - T_\infty}{T_w - T_\infty}, \\ \eta = \sqrt{\frac{a}{\nu}} y, G = ax\sqrt{\frac{a}{\nu}} h(\eta). \end{aligned}\right\} \tag{8.2.8}$$

However, Equations (8.2.2) - (8.2.6) are translated in the following dimensional equations. The completion of the continuity equation (8.2.1) is self-evident.

$$(1 + K) f''' + ff'' - f'^2 + Kh' - M^2 f' + M^2 E = 0, \tag{8.2.9}$$

$$\left(1 + \frac{K}{2}\right) h'' + fh' - f'h - K(2h + f'') = 0, \tag{8.2.10}$$

$$\left(1 + \frac{4}{3} Rd \{1 + (\theta_w - 1)\theta\}^3\right) \theta'' + Prf\theta' + 4Rd \{1 + (\theta_w - 1)\theta\}^2 (\theta_w - 1) \theta'^2 + M^2 EcPr \left(f'^2 + E^2 - 2Ef'\right) + (1 + K) PrEcf''^2 = 0 \tag{8.2.11}$$

$$\phi'' + Sc\ f\phi' = 0, \tag{8.2.12}$$

Revised boundary conditions now

$$\left.\begin{aligned} f(0) = f_w,\ f'(0) = 1 + \gamma(1 + K(1 - n)) f''(0),\ h(0) = -nf''(0), \\ \theta'(0) = -\lambda_1 (1 - \theta(0)), \phi'(0) = -\lambda_2 (1 - \phi(0)),\ \text{at}\ \ y = 0, \\ f'(y) \to 0,\ h(y) \to 0,\ \theta(y) \to 0,\ \phi(y) \to 0,\ \text{as}\ \ y \to \infty. \end{aligned}\right\} \tag{8.2.13}$$

where $Pr = \dfrac{\mu C_P}{\kappa}$, $K = \dfrac{k}{\mu}$, $M^2 = \dfrac{\sigma B_0^2}{a\rho}$, $f_w = -(av)^{-\frac{1}{2}} v_w$, $Re_x = \dfrac{ax^2}{\nu}$, $\theta_w = \dfrac{T_w}{T_\infty}$, $Sc = \dfrac{\nu}{D_M}$, $\gamma = \alpha^* \mu \sqrt{\dfrac{a}{\nu}}$, $E = \dfrac{E_0}{U_w B_0}$, $Ec = \dfrac{U_w^2}{C_P(T_w - T_\infty)}$, $\lambda_1 = \dfrac{h_{ft}}{\kappa}\sqrt{\dfrac{\nu}{a}}$, $\lambda_2 = \dfrac{h_{fc}}{D_M}\sqrt{\dfrac{\nu}{a}}$ Coefficient of skin friction, wall couple stress, Nusselt number and Sherwood number in dimensional form are

$$C_{fx} = \frac{2\tau_w}{\rho U_w^2(x)},\ Mw_x = \frac{m_w}{\rho a^2 x^3},\ Sh_x = \frac{xq_m}{D_M(C_w - C_\infty)}, Nu_x = \frac{xq_w}{\kappa(T_w - T_\infty)} \tag{8.2.14}$$

where,

$$\tau_w = \left[(\mu + k)\frac{\partial u}{\partial y} + kG\right]_{y=0}, m_w = \gamma^* \left.\frac{\partial G}{\partial y}\right|_{y=0}, q_m = -D_M \left.\frac{\partial C}{\partial y}\right|_{y=0}, q_w = -\kappa \left.\frac{\partial T}{\partial y}\right|_{y=0}, \tag{8.2.15}$$

These quantities of physical interest take on a dimensionless equation

$$Nu_x Re_x^{-\frac{1}{2}} = -\left(1+\frac{4}{3}Rd\left(\left(\theta_w-1\right)\theta\left(0\right)+1\right)^3\right)\theta'\left(0\right),$$
$$Mw_x Re_x = \left(1+\frac{K}{2}\right)h'\left(0\right),\ \frac{1}{2}C_{fx}Re_x^{\frac{1}{2}} = \left(1+\left(1-n\right)K\right)f''\left(0\right),$$
$$Sh_x Re_x^{-\frac{1}{2}} = -\phi'\left(0\right), \quad (8.2.16)$$

8.3 Solution by Homotopy Analysis Method

Liao [120] developed Homotopy analysis method for locating resolution of the governing equations. The initial guess and auxiliary linear operator can be chosen freely in the Homotopy analysis approach.
Initial guesses are

$$f_0\left(\eta\right) = f_w + \frac{1}{1+\gamma\left(1+K(1-n)\right)}\left(1-e^{-\eta}\right),\ \theta_0\left(\eta\right) = \frac{\lambda_1}{1+\lambda_1}e^{-\eta},$$
$$h_0\left(\eta\right) = \frac{n}{1+\gamma\left(1+K(1-n)\right)}e^{-\eta},\ \phi_0\left(\eta\right) = \frac{\lambda_2}{1+\lambda_2}e^{-\eta}, \quad (8.3.1)$$

with auxiliary linear operators

$$\mathcal{L}_f = \frac{\partial^3 f}{\partial\eta^3} - \frac{\partial f}{\partial\eta},\ \mathcal{L}_h = \frac{\partial^2 h}{\partial\eta^2} - h,\ \mathcal{L}_\theta = \frac{\partial^2\theta}{\partial\eta^2} - \theta,\ \mathcal{L}_\phi = \frac{\partial^2\phi}{\partial\eta^2} - \phi, \quad (8.3.2)$$

satisfying

$$\mathcal{L}_f\left(k_1+k_2e^{\eta}+k_3e^{-\eta}\right) = 0,\quad \mathcal{L}_h\left(k_4e^{\eta}+k_5e^{-\eta}\right) = 0,$$
$$\mathcal{L}_\theta\left(k_6e^{\eta}+k_7e^{-\eta}\right) = 0,\quad \mathcal{L}_\phi\left(k_8e^{\eta}+k_9e^{-\eta}\right) = 0, \quad (8.3.3)$$

Here $k_i,\ (i=1,\ 2,\ldots,9)$ are the arbitrary constants .

8.4 Convergence Analysis

Auxiliary parameters $\hbar_f$, $\hbar_h$, $\hbar_\theta$ and $\hbar_\phi$ significantly affects the convergence and approximation rate of HAM solutions. $\hbar$-curve is plotted taking appropriate order in Figure 8.2, for this purpose. For the auxiliary parameter $\hbar_f$, Figure 8.2 clearly suggests an allowable range of $-1.6 < \hbar_f < -0.1$. We use $\hbar_f = -0.50$ in this case. Similarly, $\hbar_h = -1.17$, $\hbar_\theta = -0.22$ and $\hbar_\phi = -1.84$. Convergence of series solution with varying order of approximation is calculated in Table **??**.

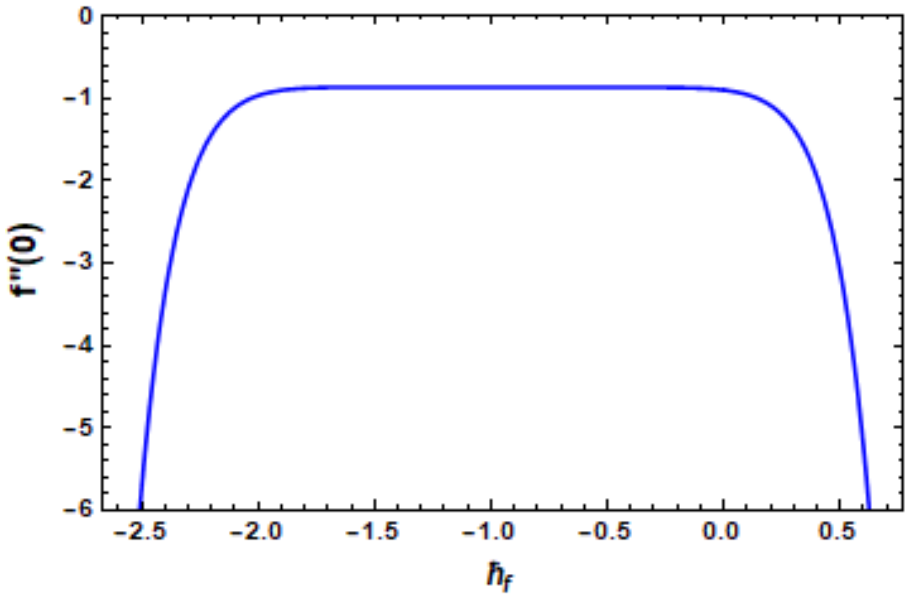

Figure 8.2: $f''(0)$ via $\hbar_f$.

8.5 Conclusion

The following are the research's findings:

- For higher values of Electric parameter and Material parameter, both increase velocity.
- With increasing values of Slip parameter, Magnetic parameter and Suction parameter, velocity decreases.
- For increasing values of Material parameter and concentration of microelements, both increase angular velocity.
- With increasing values of Prandtl number, temperature diminishes.
- For increased values of Magnetic parameter, Electric parameter, Thermal Biot number, Temperature ratio parameter, and Non-linear thermal radiation all enhance temperature.
- With higher values of Solutal Biot number raises concentration, while Schmidt number decreases it.
- For a large amount of Magnetic parameter, Skin friction coefficient increases.
- Local wall couple stress rises for a wide number of Material parameter.
- Nusselt number rises during large amount of thermal Biot number.
- Sherwood number increases for large amount of Schmidt number.

Conclusion of the Thesis

The most important findings of the work can be summerized as follows:

- Magnetic parameter M, Velocity slip parameter γ and Suction parameter f_w have retarding effects with velocity.
- Velocity profile increases with increase in Thermal Grashof number Gr_T, Solutal Grashof number Gr_C, Eckert number Ec, Electric parameter E and Micropolar parameter K.
- Weissenberg number We reduces velocity profile while variable viscosity parameter ζ behaves in opposite way.
- Angular velocity profile enhances with increase in concentration of microelements n and Micropolar parameter K, while declines with high values of unsteadiness parameter A and Thermal Grashof number Gr_T.
- Temperature of the fluid observes positive impact of Radiation parameter Rd, Magnetic parameter M, Temperature ratio parameter θ_w, Eckert number Ec and Brinkman number Br.
- A rise in temperature is observed for Heat generation/absorption coefficient β and Dufour number Du, while a decline is observed for Prandtl number Pr and Micropolar parameter K.
- For increasing values of Electric parameter E, Thermal Biot number λ_1 enhance temperature.
- Concentration field increases for Soret number Sr, Chemical reaction parameter K_c, while behaves opposite for Schimdt number Sc .
- For larger values of Suction parameter f_w, concentration decreases, while increases with increase in Solutal biot number λ_2.

- Skin friction factor enhances with increase in Weissenberg number We, velocity slip parameter γ, Thermal Grashof number Gr_T and Solutal Gashof number Gr_C whereas declined for Magnetic parameter M, Variable viscosity parameter ζ and Suction parameter f_w.

- Nusselt number is enhanced against rising values of Prandtl number Pr, temperature ratio parameter θ_w, Thermal Biot number λ_1, Thermal Grashof number Gr_T and Radiation parameter Rd, while decreases for Dufour number Du, Heat generation/absorption coefficient β and Brinkman number Br.

- Skin friction and number of Sherwood decreases for the broad unsteadiness parameter A values.

- Sherwood number is raised for Schmidt number Sc.

- N_G augmented when increment occurs in Magnetic parameter M, Diffusion parameter L^*, Thermal Grashof number Gr_T, temperature difference parmeter α_1 and Brinkman number Br.

- Bejan number has increment for large amount of α_1, L^* and M while decreases for higher values of Br.

Future Works

From studying previous research papers, it is observed that this work can be expanded in three dimensional steady and unsteady flow of Entropy optimized fluid. Also, effects of other physical parameters for different types of Non-newtonian fluids can be carried out. It may also be tried to develop a Mathematical Model of two and three dimensional blood flow with magnetic field which can be used for human life. Study of effects of Induced Magnetic field for higher dimensional Problems is rarely seen previous published works. It can also be tried to find the solutions of Magnetic field effects on blood flow with heat transfer in different types of stenosed arteries and also discussed comparative study of different types of blood flow of different type's stenosed arteries

Published/Accepted Research Articles

1. H. R. Kataria, M. H. Mistry, Effect of Non-linear Radiation on MHD Mixed Convection Flow of a Micropolar fluid Over an Unsteady Stretching Sheet. In **Journal of Physics**, (2021), 1964, p. 022005, ISSN : 1742-6596. doi:10.1088/1742-6596/1964/2/022005, **(Scopus).**

2. H. R. Kataria, M. H. Mistry, A. S. Mittal, Influence of nonlinear radiation on MHD Micropolar fluid flow with viscous dissipation, **Heat Transfer (Wiley)**, (2022), 51(2), 1449-1467, ISSN : 2688-4542. https://doi.org/10.1002/htj.22359, **(Scopus)**.

3. H. R. Kataria, M. H. Mistry, Entropy optimized MHD fluid flow over a vertical stretching sheet in presence of radiation, **Heat Transfer (Wiley)**, (2022), 51(3), 2546-2564, ISSN : 2688-4542. https://doi.org/10.1002/htj.22412, **(Scopus)**.

4. H. R. Kataria, A. S. Mittal, M. H. Mistry, Effect of nonlinear radiation on entropy optimised MHD fluid flow, **International Journal of Ambient Energy (Taylor and Fransis)**, (2022), 1-10, ISSN : 2162-8246. https://doi.org/10.1080/01430750.2022.2059000, **(Scopus).**

5. H. R. Kataria, A. S. Mittal, M. H. Mistry, Consequences of nonlinear radiation, variable viscosity, Soret and Dufour effects on MHD Carreau fluid flow, **International Journal of Applied and Computational Mathematics (Springer)**, (2022), ISSN : 2199-5796, **(Scopus).**

Communicated Research Work

1. H. R. Kataria, M. H. Mistry, A. S. Mittal, Soret and Dufour impact on MHD Williamson fluid flow with non linear radiation and varying viscosity.

2. H. R. Kataria, M. H. Mistry, Entropy optimized unsteady MHD natural convective flow of Williamson fluid including onlinear radiation and viscous dissipation effects.

Presented Research Work in Conferences

1. M. H. Mistry, H. R. Kataria, Mathematical Modelling of two dimensional electrically conducting Williamson fluid considering variable viscosity and radiation, in YOUNG SCIENTIST CONFERENCE as a part of India International Science Festival-2019 held at Biswa Bangla Convention Centre, Kolkata during November 5-8, 2019.

2. M. H. Mistry, H. R. Kataria, Mathematical modelling of two dimensional magnetohydrodynamic fluid flow considering variable viscosity and radiation, at the Science Conclave 2020 organized by Faculty of Science, The Maharaja Sayajirao University of Baroda, Vadodara on 28th February 2020.

3. M. H. Mistry, H. R. Kataria, Magneto-Micropolar electrically conducting fluid flow over a linearly stretching sheet for heat and mass transfer in International conference on Advances in Differential equations and Numerical analysis organized by Department of Mathematics, Indian Institute of Technology, Guwahati, India during October 12-15, 2020.

4. M. H. Mistry, H. R. Kataria, Effect of radiation on two dimensional electrically conducting Williamson fluid considering variable viscosity in the 21st International conference on Science, Engineering and Technology (ISCET-2020), organized by Vellore Institute of Technology, Vellore during November 30, 2020 to December 1, 2020.

5. M. H. Mistry, H. R. Kataria, Influence of Variable Thermal Conductivity and Viscosity on MHD Boundary Layer Flow of Carreau Fluid Over Stretching/Shrinking Sheet in the International Science Symposium on Recent trends in Science and Technology, organized by Christ college, Rajkot on 8th and 9th, April 2021. I stood second in the competition.

6. M. H. Mistry, H. R. Kataria, Entropy optimized MHD natural convective flow of Williamson fluid with nonlinear radiation and viscous dissipation effects,

International Conference on Recent Advances in Fluid Mechanics (ICRAFM-2022) organized Manipal Institute of Technology, MAHE, Manipal on 4th-6th, October 2022.

Bibliography

[1] A. Ajibade, A. Umar, Effects of viscous dissipation and boundary wall thickness on steady natural convection Couette flow with variable viscosity and thermal conductivity, International Journal of Thermofluids, 7(2020) 100052. https://doi.org/10.1016/j.ijft.2020.100052.

[2] A. A. Afify, MHD free convective flow and mass transfer over a stretching sheet with chemical reaction, Heat and Mass Transfer, 40(2004) 495-500. https://doi.org/10.1007/s00231-003-0486-0.

[3] A. T. Akinshilo, Mixed convective heat transfer analysis of MHD fluid flowing through an electrically conducting and non-conducting walls of a vertical micro-channel considering radiation effect, Applied Thermal Engineering, 156(2019) 506-513. https://doi.org/10.1016/j.applthermaleng.2019.04.100.

[4] A. Bejan, A study of entropy generation in fundamental convective heat transfer, Journal of heat transfer, 101(1979) 718-725. https://doi.org/10.1115/1.3451063.

[5] A. Bejan, Second law analysis in heat transfer, Energy, 5(1980) 720-732. https://doi.org/10.1016/0360-5442(80)90091-2.

[6] A. Borrelli, G. Giantesio, M. C. Patria, N. C. Roşca, A. V. Roşca, I. Pop, Buoyancy effects on the 3D MHD stagnation-point flow of a Newtonian fluid, Communications in Nonlinear Science and Numerical Simulation, 43(2017) 1-13. https://doi.org/10.1016/j.cnsns.2016.06.022.

[7] A. Chamkha, Mass transfer with chemical reaction in MHD mixed convective flow along a vertical stretching sheet, International Journal of Energy & Technology, 4(2012) 1-12.

[8] A. J. Chamkha, A. M. Rashad, Unsteady heat and mass transfer by MHD mixed convection flow from a rotating vertical cone with chemical reaction

and Soret and Dufour effects, The Canadian Journal of Chemical Engineering, 92(2014) 758-767. https://doi.org/10.1002/cjce.21894.

[9] A. C. Eringen, Theory of micropolar fluids, Journal of mathematics and Mechanics, 16(1966) 1-18. https://www.jstor.org/stable/24901466.

[10] A. C. Eringen, Theory of thermomicrofluids, Journal of Mathematical analysis and Applications, 38(1972) 480-496. https://doi.org/10.1016/0022-247X(72)90106-0.

[11] A. Idowu, M. Akolade, J. Abubakar, B. Falodun, MHD free convective heat and mass transfer flow of dissipative Casson fluid with variable viscosity and thermal conductivity effects, Journal of Taibah University for Science, 14(2020) 851-862. https://doi.org/10.1080/16583655.2020.1781431.

[12] A. Ishak, Unsteady MHD flow and heat transfer over a stretching plate, Journal of Applied Sciences, 10(2010) 2127-2131. https://dx.doi.org/10.3923/jas.2010.2127.2131.

[13] A. V. Lemoff, A. P. Lee, An AC magnetohydrodynamic micropump, Sensors and Actuators B: Chemical, 63(2000) 178–185. https://doi.org/10.1016/S0925-4005(00)00355-5.

[14] A. S. Mittal, H. R. Patel, R. R. Darji, Mixed Convection Micropolar Ferrofluid Flow with Viscous Dissipation, Joule Heating and Convective Boundary Conditions, International Communications in Heat and Mass Transfer, 108(2019) 104320. https://doi.org/10.1016/j.icheatmasstransfer.2019.104320.

[15] A. S. Mittal, H. R. Kataria, Three dimensional CuO–Water nanofluid flow considering Brownian motion in presence of radiation, Karbala International Journal of Modern Science, 4(2018) 275-286. https://doi.org/10.1016/j.kijoms.2018.05.002.

[16] A. S. Mittal, H. R. Patel, Influence of thermophoresis and Brownian motion on mixed convection two dimensional MHD Casson fluid flow with non-linear radiation and heat generation, Physica A: Statical Mechanicsa and its Applications, 537(2020) 122710. https://doi.org/10.1016/j.physa.2019.122710.

[17] A. M. Rashad, S. Abbasbandy, A. J. Chamkha, Mixed convection flow of a micropolar fluid over a continuously moving vertical surface immersed in

a thermally and solutally stratified medium with chemical reaction, Journal of the Taiwan Institute of Chemical Engineers, 45(2014) 2163-2169. https://doi.org/10.1016/j.jtice.2014.07.002.

[18] A. Raptis, A. K. Singh, MHD free convection flow past an accelerated vertical plate, International Communications in Heat and Mass Transfer, 10(1983) 313-321. https://doi.org/10.1016/0735-1933(83)90016-7.

[19] A. Ullah, A. Hafeez, W. K. Mashwani, W. Kumam, P. Kumam, M. Ayaz, Non-linear thermal radiations and mass transfer analysis on the processes of magnetite carreau fluid flowing past a permeable stretching/shrinking surface under cross diffusion and Hall effect, Coatings, 10(2020) 523. https://doi.org/10.3390/coatings10060523.

[20] B. J. Gireesha, A. Roja, Second law analysis of MHD natural convection slip flow of Casson fluid through an inclined microchannel, Multidiscipline Modeling in Materials and Structures, 16(2020) 1435-1455. https://doi.org/10.1108/MMMS-11-2019-0189.

[21] B. Gireesha, M. Umeshaiah, B. Prasannakumara, N. Shashikumar, M. Archana, Impact of nonlinear thermal radiation on magnetohydrodynamic three dimensional boundary layer flow of Jeffrey nanofluid over a nonlinearly permeable stretching sheet, Physica A: Statistical Mechanics and its Applications, 549(2020) 124051. https://doi.org/10.1016/j.physa.2019.124051.

[22] B. Gireesha, M. Archana, P. Kumar, R. Gorla, Significance of temperature dependent viscosity, nonlinear thermal radiation and viscous dissipation on the dynamics of water conveying cylindrical and brick shaped molybdenum disulphide nanoparticles, International Journal of Applied and Computational Mathematics, 5(2019) 1-15. https://doi.org/10.1007/s40819-019-0649-4.

[23] B. Raftari, K. Vajravelu, Homotopy analysis method for MHD viscoelastic fluid flow and heat transfer in a channel with a stretching wall, Communications in nonlinear science and numerical simulation, 17(2012) 4149-4162. https://doi.org/10.1016/j.cnsns.2012.01.032.

[24] B. K. Swain, B. C. Parida, S. Kar, N. Senapati, Viscous dissipation and joule heating effect on MHD flow and heat transfer past a stretching sheet embedded in a porous medium, Heliyon, 6(2020) e05338. https://doi.org/10.1016/j.heliyon.2020.e05338.

[25] C. C. Cho, Mixed convection heat transfer and entropy generation of Cu-water nanofluid in wavy-wall lid-driven cavity in presence of inclined magnetic field, International Journal of Mechanical Sciences, 151(2019) 703-714. https://doi.org/10.1016/j.ijmecsci.2018.12.017.

[26] C. J. Huang, Influence of non-Darcy and MHD on free convection of non-Newtonian fluids over a vertical permeable plate in a porous medium with soret/dufour effects and thermal radiation, International Journal of Thermal Sciences, 130(2018) 256-263. https://doi.org/10.1016/j.ijthermalsci.2018.04.019.

[27] D. D. Gray, A. Giorgini, The validity of the Boussinesq approximation for liquids and gases, International Journal of Heat and Mass Transfer, 19(1976) 545-551. https://doi.org/10.1016/0017-9310(76)90168-X.

[28] D. Pal, G. Mandal, K. Vajravalu, Soret and Dufour effects on MHD convective–radiative heat and mass transfer of nanofluids over a vertical non-linear stretching/shrinking sheet, Applied Mathematics and Computation, 287(2016) 184-200. https://doi.org/10.1016/j.amc.2016.04.037.

[29] F. Mabood, W. A. Khan, A. I. M. Ismail, Approximate analytical modeling of heat and mass transfer in hydromagnetic flow over a non-isothermal stretched surface with heat generation/absorption and transpiration, Journal of the Taiwan Institute of Chemical Engineers, 54(2015) 11-19. https://doi.org/10.1016/j.jtice.2015.03.022.

[30] F. Mabood, T. Yusuf, G. Bognár, Features of entropy optimization on MHD couple stress nanofluid slip flow with melting heat transfer and nonlinear thermal radiation, Scientific Reports, 10(2020) 1-13. https://doi.org/10.1038/s41598-020-76133-y.

[31] F. Sultan, S. Mustafa, W. Khan, M. Shahzad, M. Ali, W. Adnan, S. Rehman, A numerical treatment on rheology of mixed convective Carreau nanofluid with variable viscosity and thermal conductivity, Applied Nanoscience, 10(2020) 3295-3303. https://doi.org/10.1007/s13204-020-01294-1.

[32] F. A. Soomro, M. Usman, R. U. Haq, W. Wang, Thermal and velocity slip effects on MHD mixed convection flow of Williamson nanofluid along a vertical surface: Modified Legendre wavelets approach, Physica E: Low-dimensional Systems and Nanostructures, 104(2018) 130-137. https://doi.org/10.1016/j.physe.2018.07.002.

[33] F. Selimefendigil, H. F. Öztop, MHD mixed convection and entropy generation of power law fluids in a cavity with a partial heater under the effect of a rotating cylinder, International Journal of Heat and Mass Transfer, 98(2016) 40-51. https://doi.org/10.1016/j.ijheatmasstransfer.2016.02.092.

[34] F. Wang, M. I. Asjad, M. Zahid, A. Iqbal, H. Ahmad, M. D. Alsulami, Unsteady Thermal Transport Flow of Casson Nanofluids with Generalized Mittag–Leffler Kernel of Prabhakar's Type, Journal of Materials Research and Technology, 14(2021) 1292–1300. https://doi.org/10.1016/j.jmrt.2021.07.029.

[35] G. Lukaszewicz, Micropolar fluids: theory and applications, Springer Science & Business Media, (1999).

[36] G. Nagaraju, J. Srinivas, J. R. Murthy, A. M. Rashad, Entropy generation analysis of the MHD flow of couple stress fluid between two concentric rotating cylinders with porous lining, Heat Transfer-Asian Research, 46(2017) 316-330. https://doi.org/10.1002/htj.21214.

[37] G. J. Reddy, R. S. Raju, J. A. Rao, Influence of viscous dissipation on unsteady MHD natural convective flow of Casson fluid over an oscillating vertical plate via FEM, Ain Shams Engineering Journal, 9(2018) 1907-1915. https://doi.org/10.1016/j.asej.2016.10.012.

[38] H. R. Patel, A. S. Mittal, R. R. Darji, MHD Flow of Micropolar Nanofluid over a Stretching/Shrinking Sheet Considering Radiation, International Communications in Heat and Mass Transfer, 108(2019) 104322. https://doi.org/10.1016/j.icheatmasstransfer.2019.104322.

[39] H. R. Kataria, A. S. Mittal, Mathematical model for velocity and temperature of gravity-driven convective optically thick nanofluid flow past an oscillating vertical plate in presence of magnetic field and radiation, Journal of Nigerian Mathematical Society, 34(2015) 303-317. https://doi.org/10.1016/j.jnnms.2015.08.005.

[40] H. R. Kataria, A. S. Mittal, Velocity, Mass and Temperature Analysis of Gravity-Driven Convection Nanofluid Flow Past an Oscillating Vertical Plate in the Presence of Magnetic Field in a Porous Medium, Applied Thermal Engineering, 110(2017a) 864-874. https://doi.org/10.1016/j.applthermaleng.2016.08.129.

[41] H. R. Kataria, H. R. Patel, Radiation and chemical reaction effects on MHD Casson fluid flow past an oscillating vertical plate embedded in porous medium, Alexandria Engineering Journal, 55(2016) 583-595. https://doi.org/10.1016/j.aej.2016.01.019.

[42] H. R. Kataria, H. R. Patel, Soret and heat generation effects on MHD Casson fluid flow past an oscillating vertical plate embedded through porous medium, Alexandria Engineering Journal, 55(2016) 2125-2137. https://doi.org/10.1016/j.aej.2016.06.024.

[43] H. R. Kataria, H. R. Patel, Effects of chemical reaction and heat generation/absorption on magnetohydrodynamic (MHD) Casson fluid flow over an exponentially accelerated vertical plate embedded in porous medium with ramped wall temperature and ramped surface concentration, Propulsion and Power Research 8(2019) 35-46. https://doi.org/10.1016/j.jppr.2018.12.001.

[44] H. R. Kataria, H. R. Patel, R. Singh, Effect of magnetic field on unsteady natural convective flow of a micropolar fluid between two vertical walls, Ain Shams Engineering Journal, 8(2017) 87-102. https://doi.org/10.1016/j.asej.2015.08.013.

[45] H. Kataria, H. Patel, Effect of thermo-diffusion and parabolic motion on MHD Second grade fluid flow with ramped wall temperature and ramped surface concentration, Alexandria engineering journal, 57(2018) 73-85. https://doi.org/10.1016/j.aej.2016.11.014.

[46] H. F. Öztop, N. S. Bondareva, M. A. Sheremet, N. Abu-Hamdeh, Unsteady natural convection with entropy generation in partially open triangular cavities with a local heat source, International Journal of Numerical Methods for Heat & Fluid Flow, 27(2017) 2696-2716. https://doi.org/10.1108/HFF-12-2016-0510.

[47] H. S. Takhar, A. A. Raptis, C. P. Perdikis, MHD asymmetric flow past a semi-infinite moving plate, Acta Mechanica, 65(1987) 287-290. https://doi.org/10.1007/BF01176888.

[48] H. Vaidya, C. Rajashekhar, F. Mebarek-Oudina, K. V. Prasad, K. Vajravelu, B. Ramesh Bhat, Examination of Chemical Reaction on Three Dimensional Mixed Convective Magnetohydrodynamic Jeffrey Nanofluid Over a Stretching Sheet, Journal of Nanofluids, 11(2022) 113-124. https://doi.org/10.1166/jon.2022.1817.

[49] J. Hartmann, Hg-dynamics I theory of the laminar flow of an electrically conductive liquid in a homogenous magnetic field, Det Kal. Danske Vidensk-abernes selskab, Mathematisk-fysiske Meddeleser, 15(1937) 1-27.

[50] J. Wang, R. Muhammad, M. I. Khan, W. A. Khan, S. Z. Abbas, Entropy optimized MHD nanomaterial flow subject to variable thicked surface, Computer Methods and Programs in Biomedicine, 189(2020) 105311. https://doi.org/10.1016/j.cmpb.2019.105311.

[51] J. Zhong, M. Yi, H. H. Bau, Magnetohydrodynamic (MHD) pump fabricated with ceramic tapes, Sensors and Actuators A: Physical, 96(2002) 59–66. https://doi.org/10.1016/S0924-4247(01)00764-6.

[52] K. Anantha Kumar, V. Sugunamma, N. Sandeep, Physical aspects on unsteady MHD-free convective stagnation point flow of micropolar fluid over a stretching surface, Heat Transfer—Asian Research, 48(2019) 3968-3985. https://doi.org/10.1002/htj.21577.

[53] K. Aslani, U. S. Mahabaleshwar, J. Singh, I. E. Sarris, Combined effect of radiation and inclined MHD flow of a micropolar fluid over a porous stretching/shrinking sheet with mass transpiration, International Journal of Applied and Computational Mathematics, 7(2021) 1-21. https://doi.org/10.1007/s40819-021-00987-7.

[54] K. Batchlor, An introduction to fluid dynamics, London: Cambridge University Press, 158(1987).

[55] K. G. Kumar, G. K. Ramesh, B. J. Gireesha, R. S. R. Gorla, Characteristics of Joule heating and viscous dissipation on three-dimensional flow of Oldroyd B nanofluid with thermal radiation, Alexandria Engineering Journal, 57(2018) 2139-2149. https://doi.org/10.1016/j.aej.2017.06.006.

[56] K. Jabeen, M. Mushtaq, R. M. A. Muntazir, Analysis of MHD Fluids around a Linearly Stretching Sheet in Porous Media with Thermophoresis, Radiation and Chemical Reaction, Mathematical Problems in Engineering, 2020(2020) 9685482. https://doi.org/10.1155/2020/9685482.

[57] K. L. Hsiao, Combined electrical MHD heat transfer thermal extrusion system using Maxwell fluid with radiative and viscous dissipation effects, Applied Thermal Engineering, 112(2017) 1281-1288. https://doi.org/10.1016/j.applthermaleng.2016.08.208.

[58] K. R. Rajagopal, M. Ruzicka, A. R. Srinivasa, On the Oberbeck-Boussinesq approximation, Mathematical Models and Methods in Applied Sciences, 6(1996). 1157-1167. https://doi.org/10.1142/S0218202596000481.

[59] K. U. Rehman, A. S. Alshomrani, M. Y. Malik, Carreau fluid flow in a thermally stratified medium with heat generation/absorption effects, Case studies in thermal engineering, 12(2018) 16-25. https://doi.org/10.1016/j.csite.2018.03.001.

[60] K. Sarada, R. J. P. Gowda, I. E. Sarris, R. N. Kumar, B. C. Prasannakumara, Effect of Magnetohydrodynamics on Heat Transfer Behaviour of a Non-Newtonian Fluid Flow over a Stretching Sheet under Local Thermal Non-Equilibrium Condition, Fluids, 6(2021) 264. https://doi.org/10.3390/fluids6080264.

[61] K. Sharma, K. Bhaskar, Influence of Soret and Dufour on Three-Dimensional MHD Flow Considering Thermal Radiation and Chemical Reaction, International Journal of Applied and Computational Mathematics, 6(2020) 1-17. https://doi.org/10.1007/s40819-019-0753-5.

[62] K. A. Yih, Free convection effect on MHD coupled heat and mass transfer of a moving permeable vertical surface, International Communications in Heat and Mass Transfer, 26(1999) 95-104. https://doi.org/10.1016/S0735-1933(98)00125-0.

[63] L. A. Lund, Z. Omar, S. Dero, I. Khan, Linear stability analysis of MHD flow of micropolar fluid with thermal radiation and convective boundary condition: Exact solution, Heat Transfer—Asian Research, 49(2020) 461-476. https://doi.org/10.1002/htj.21621.

[64] M. S. Astanina, M. A. Sheremet, H. F. Öztop, N. Abu-Hamdeh, MHD natural convection and entropy generation of ferrofluid in an open trapezoidal cavity partially filled with a porous medium, International Journal of Mechanical Sciences, 136(2018) 493-502. https://doi.org/10.1016/j.ijmecsci.2018.01.001.

[65] M. Bibi, A. Zeeshan, M. Malik, Numerical analysis of unsteady flow of three-dimensional Williamson fluid-particle suspension with MHD and nonlinear thermal radiations, The European Physical Journal Plus, 135(2020) 1-26. https://doi.org/10.1140/epjp/s13360-020-00857-z.]

[66] M. Bhatti, L. Phali, C. M. Khalique, Heat transfer effects on electro-magnetohydrodynamic Carreau fluid flow between two micro-parallel plates with Darcy-Brinkman-Forchheimer medium, Archive of Applied Mechanics, 91(2021) 1683-1695. https://doi.org/10.1007/s00419-020-01847-4.

[67] M. Dada, C. Onwubuoya, Variable viscosity and thermal conductivity effects on Williamson fluid flow over a slendering stretching sheet, World Journal of Engineering, 17(2020) 357-371. https://doi.org/10.1108/WJE-08-2019-0222.

[68] M. F. El-Amin, Magnetohydrodynamic free convection and mass transfer flow in micropolar fluid with constant suction, Journal of magnetism and magnetic materials, 234(2001) 567-574. https://doi.org/10.1016/S0304-8853(01)00374-2.

[69] M. Farooq, M. I. Khan, M. Waqas, T. Hayat, A. Alsaedi, M. I. Khan, MHD Stagnation Point Flow of Viscoelastic Nanofluid with Non-Linear Radiation Effects, Journal of Molecular Liquids, 221(2016) 1097–1103. https://doi.org/10.1016/j.molliq.2016.06.077.

[70] M. A. Hossain, Viscous and Joule heating effects on MHD free convection flow with variable plate temperature (No. IC–90/265). International Centre for Theoretical Physics, (1990).

[71] M. Hussain, A. Ghaffar, A. Ali, A. Shahzad, K. Nisar, M. Alharthi, W. Jamshed, MHD thermal boundary layer flow of a Casson fluid over a penetrable stretching wedge in the existence of nonlinear radiation and convective boundary condition, Alexandria Engineering Journal, 60(2021) 5473-5483. https://doi.org/10.1016/j.aej.2021.03.042.

[72] M. Imtiaz, H. Nazar, T. Hayat, A. Alsaedi, Soret and Dufour effects in the flow of viscous fluid by a curved stretching surface, Pramana, 94(2020) 1-11. https://doi.org/10.1007/s12043-020-1922-0.

[73] M. Kayalvizhi, R. Kalaivanan, N. V. Ganesh, B. Ganga, A. A. Hakeem, Velocity slip effects on heat and mass fluxes of MHD viscous–Ohmic dissipative flow over a stretching sheet with thermal radiation, Ain Shams Engineering Journal, 7(2016) 791-797. https://doi.org/10.1016/j.asej.2015.05.010.

[74] M. I. Khan, F. Alzahrani, Activation Energy and Binary Chemical Reaction Effect in Nonlinear Thermal Radiative Stagnation Point Flow of Walter-B Nanofluid: Numerical Computations, International Journal of Modern Physics B, 34(2020) 2050132. https://doi.org/10.1142/S0217979220501325.

[75] M. I. Khan, A. Kumar, T. Hayat, M. Waqas, R. Singh, Entropy generation in flow of Carreau nanofluid, Journal of Molecular Liquids, 278(2019) 677-687. https://doi.org/10.1016/j.molliq.2018.12.109.

[76] M. V. Krishna, K. Vajravelu, Hall effects on the unsteady MHD flow of the Rivlin–Ericksen fluid past an infinite vertical porous plate, Waves in Random and Complex Media, (2022)1-24. https://doi.org/10.1080/17455030.2022.2084178.

[77] M. Massoudi, I. Christie, Effects of variable viscosity and viscous dissipation on the flow of a third grade fluid in a pipe, International Journal of Non-Linear Mechanics, 30(1995) 687-699. https://doi.org/10.1016/0020-7462(95)00031-I.

[78] M. Madhu, B. Mahanthesh, N. S. Shashikumar, S. A. Shehzad, S. U. Khan, B. J. Gireesha, Performance of second law in Carreau fluid flow by an inclined microchannel with radiative heated convective condition, International Communications in Heat and Mass Transfer. 117(2020) 104761. https://doi.org/10.1016/j.icheatmasstransfer.2020.104761.

[79] M. K. Nayak, A. A. Hakeem, B. Ganga, M. I. Khan, M. Waqas, O. D. Makinde, Entropy optimized MHD 3D nanomaterial of non-Newtonian fluid: a combined approach to good absorber of solar energy and intensification of heat transport, Computer methods and programs in biomedicine, 186(2020) 105131. https://doi.org/10.1016/j.cmpb.2019.105131.

[80] M. K. Nayak, S. Shaw, A.J. Chamkha, 3D MHD Free Convective Stretched Flow of a Radiative Nanofluid Inspired by Variable Magnetic Field, Arabian Journal of science and engineering, 44(2019) 1269-1282. https://doi.org/10.1007/s13369-018-3473-y.

[81] M. K. Nayak,N. S. Akbar, D. Tripathi, V. S. Pandey, Three dimensional MHD flow of nanofluid over an exponential porous stretching sheet with convective boundary conditions, Thermal Science and Engineering Progress, 3(2017) 133-140. https://doi.org/10.1016/j.tsep.2017.07.006.

[82] M. K. Nayak, G. C. Dash, L. P. Singh, Heat and mass transfer effects on MHD viscoelastic fluid over a stretching sheet through porous medium in presence of chemical reaction, Propulsion and Power Research, 5(2016) 70-80. https://doi.org/10.1016/j.jppr.2016.01.006.

[83] M. Ramzan, M. Farooq, T. Hayat, J. D. Chung, Radiative and Joule heating effects in the MHD flow of a micropolar fluid with partial slip and convective boundary condition, Journal of Molecular Liquids, 221(2016) 394-400. https://doi.org/10.1016/j.molliq.2016.05.091.

[84] M. M. Rashidi, S. Abelman, N. F. Mehr, Entropy generation in steady MHD flow due to a rotating porous disk in a nanofluid, International journal of Heat and Mass transfer, 62(2013) 515-525. https://doi.org/10.1016/j.ijheatmasstransfer.2013.03.004.

[85] M. M. Rashidi, B. Rostami, N. Freidoonimehr, S. Abbasbandy, Free convective heat and mass transfer for MHD fluid flow over a permeable vertical stretching sheet in the presence of the radiation and buoyancy effects, Ain Shams Engineering Journal, 5(2014) 901-912. https://doi.org/10.1016/j.asej.2014.02.007.

[86] M. M. Rashidi, S. A. Mohimanian Pour, A novel analytical solution of heat transfer of a micropolar fluid through a porous medium with radiation by DTM-Padé, Heat Transfer-Asian Research, 39(2010) 575-589. https://doi.org/10.1002/htj.20317.

[87] M. G. Reddy, P. Padma, B. Shankar, Effects of viscous dissipation and heat source on unsteady MHD flow over a stretching sheet, Ain Shams Engineering Journal, 6(2015) 1195-1201. https://doi.org/10.1016/j.asej.2015.04.006.

[88] M. Sheikholeslami, H. R. Kataria, A. S. Mittal, Radiation Effects on Heat Transfer of Three Dimensional Nanofluid Flow Considering Thermal Interfacial Resistance and Micro Mixing in Suspensions, Chinese Journal of Physics, 55(2017) 2254–2272. https://doi.org/10.1016/j.cjph.2017.09.010.

[89] M. Sheikholeslami, H. R. Kataria, A. S. Mittal, Effect of thermal diffusion and heat-generation on MHD nanofluid flow past an oscillating vertical plate through porous medium, Journal of Molecular Liquids, 257(2018) 12-25. https://doi.org/10.1016/j.molliq.2018.02.079.

[90] M. Sheikholeslami, D. D. Ganji, M. Y. Javed, R. Ellahi, Effect of thermal radiation on magnetohydrodynamics nanofluid flow and heat transfer by means of two phase model, Journal of magnetism and Magnetic materials, 374(2015) 36-43. https://doi.org/10.1016/j.jmmm.2014.08.021.

[91] M. Sulemana, I. Y. Seini, O. D. Makinde, Hydrodynamic Boundary Layer Flow of Chemically Reactive Fluid over Exponentially Stretching Vertical Surface with Transverse Magnetic Field in Unsteady

Porous Medium, Journal of Applied Mathematics, 2022(2022) 7568695. https://doi.org/10.1155/2022/7568695.

[92] M. Turkyilmazoglu, MHD fluid flow and heat transfer due to a stretching rotating disk, International journal of thermal sciences, 51(2012) 195-201. https://doi.org/10.1016/j.ijthermalsci.2011.08.016.

[93] M. Turkyilmazoglu, I. Pop, Exact analytical solutions for the flow and heat transfer near the stagnation point on a stretching/shrinking sheet in a Jeffrey fluid, International Journal of Heat and Mass Transfer, 57(2013) 82-88. https://doi.org/10.1016/j.ijheatmasstransfer.2012.10.006.

[94] M. Turkyilmazoglu, MHD fluid flow and heat transfer due to a shrinking rotating disk, Computers & Fluids, 90(2014) 51-56. https://doi.org/10.1016/j.compfluid.2013.11.005.

[95] M. Usman, Z. H. Khan, M. B. Liu, MHD natural convection and thermal control inside a cavity with obstacles under the radiation effects, Physica A: Statical Mechanics and its applications, 535(2019) 122443. https://doi.org/10.1016/j.physa.2019.122443.

[96] M. Waqas, M. Farooq, M. I. Khan, A. Alsaedi, T. Hayat, T. Yasmeen, Magnetohydrodynamic (MHD) mixed convection flow of micropolar liquid due to nonlinear stretched sheet with convective condition, International Journal of Heat and Mass Transfer, 102(2016) 766-772. https://doi.org/10.1016/j.ijheatmasstransfer.2016.05.142.

[97] N. Kumar, S. Gupta, MHD free-convective flow of micropolar and Newtonian fluids through porous medium in a vertical channel, Meccanica, 47(2012) 277-291. https://doi.org/10.1007/s11012-011-9435-z.

[98] N. K. Ranjit, G. C. Shit, Entropy generation on electromagnetohydrodynamic flow through a porous asymmetric micro-channel, European Journal of Mechanics-B/Fluids, 77(2019) 135–147. https://doi.org/10.1016/j.euromechflu.2019.05.002.

[99] N. R. Devi, M. Shivananda, H. F. Öztop, N. Abu-Hamdeh, P. Padmanathan, A. Satheesh, A review on ferrofluids with the effect of MHD and entropy generation due to convective heat transfer, The European Physical Journal Plus, 137(2022) 482. https://doi.org/10.1140/epjp/s13360-022-02616-8.

[100] N. Z. Basha, K. Vajravelu, F. Mebarek-Oudina, I. Sarris, K. Vaidya, K. V. Prasad, C. Rajashekhar, MHD Carreau nanoliquid flow over a nonlinear stretching surface, Heat Transfer, 51(2022) 5262-5287. https://doi.org/10.1002/htj.22546.

[101] O. A. Bég, A. Y. Bakier, V. R. Prasad, Numerical study of free convection magnetohydrodynamic heat and mass transfer from a stretching surface to a saturated porous medium with Soret and Dufour effects, Computational Materials Science, 46 (2009) 57-65. https://doi.org/10.1016/j.commatsci.2009.02.004.

[102] P. J. Carreau, D. Kee, M. Daroux, An analysis of the viscous behaviour of polymeric solutions, The Canadian Journal of Chemical Engineering, 57(1979) 135-140. https://doi.org/10.1002/cjce.5450570202.

[103] P. S. Reddy, A. J. Chamkha, A. Al-Mudhaf, MHD heat and mass transfer flow of a nanofluid over an inclined vertical porous plate with radiation and heat generation/absorption, Advanced Powder Technology, 28(2017) 1008-1017. https://doi.org/10.1016/j.apt.2017.01.005.

[104] P. G. Siddheshwar, U. S. Mahabaleswar, H. I. Andersson, A new analytical procedure for solving the non-linear differential equation arising in the stretching sheet problem, International Journal of Applied Mechanics and Engineering, 18(2013) 955-964. https://doi.org/10.2478/ijame-2013-0059.

[105] P. G. Siddheshwar, A. Chan, U. S. Mahabaleswar, Suction-induced magnetohydrodynamics of a viscoelastic fluid over a stretching surface within a porous medium, The IMA Journal of Applied Mathematics, 79(2014) 445-458. https://doi.org/10.1093/imamat/hxs074.

[106] R. C. Chaudhary, A. K. Jha, Effects of chemical reactions on MHD Micropolar fluid flow past a vertical plate in slip-flow regime, Applied mathematics and Mechanics, 29(2008) 1179-1194. https://doi.org/10.1007/s10483-008-0907-x.

[107] R. J. P. Gowda, R. N. Kumar, A. M. Jyothi, B. C. Prasannakumara, I. E. Sarris, Impact of Binary Chemical Reaction and Activation Energy on Heat and Mass Transfer of Marangoni Driven Boundary Layer Flow of a Non-Newtonian Nanofluid, Processes, 9(2021) 702. https://doi.org/10.3390/pr9040702.

[108] R. Mehta, H. R. Kataria, Brownian motion and thermophoresis effects on MHD flow of viscoelastic fluid over stretching/shrinking sheet in the presence of thermal radiation and chemical reaction, Heat Transfer, 51(2022) 274-295. https://doi.org/10.1002/htj.22307.

[109] R. Saravana, R. Hemadri Reddy, K. V. Narasimha Murthy, O. D. Makinde, Thermal radiation and diffusion effects in MHD Williamson and Casson fluid flows past a slendering stretching surface, Heat Transfer, 51(2022) 3187-3200. https://doi.org/10.1002/htj.22443.

[110] R. V. Williamson, The flow of pseudoplastic materials, Industrial & Engineering Chemistry, 21(1929), 1108-1111. https://doi.org/10.1021/ie50239a035.

[111] S. Abbasbandy, Homotopy analysis method for heat radiation equations. International Communications in Heat and Mass Transfer, 34(2007) 380–387. https://doi.org/10.1016/j.icheatmasstransfer.2006.12.001.

[112] S. K. Adegbie, O. K. Koriko, I. L. Animasaun, Melting heat transfer effects on stagnetion point flow of micropolar fluid with variable dynamic viscosity and thermal conductivity at constant vortex viscosity, Journal of the Nigerian Mathematical society, 35(2016) 34-47. http://dx.doi.org/10.1016/j.jnnms.2015.06.004.

[113] S. Afsana, M. M. Molla, P. Nag, L. K. Saha, S. Siddiqa, MHD Natural Convection and Entropy Generation of non-Newtonian Ferrofluid in a Wavy Enclosure, International Journal of Mechanical Sciences, 198(2021) 106350. https://doi.org/10.1016/j.ijmecsci.2021.106350.

[114] S. M. Arifuzzaman, M. S. Khan, M. F. U. Mehedi, B. M. J. Rana, S.F. Ahmmed, Chemically reactive and naturally convective high speed MHD fluid flow through an oscillatory vertical porous plate with heat and radiation absorption effect, Engineering Science and Technology, an International Journal, 21(2018) 215-228. https://doi.org/10.1016/j.jestch.2018.03.004.

[115] S. Das, R. N. Jana, O. D. Makinde, MHD boundary layer slip flow and heat transfer of nanofluid past a vertical stretching sheet with non-uniform heat generation/absorption, International Journal of Nanoscience, 13(2014), 1450019. https://doi.org/10.1142/S0219581X14500197.

[116] S. Das, R. N. Jana, O. D. Makinde, Magnetohydrodynamic mixed convective slip flow over an inclined porous plate with viscous dissipation and Joule heating. Alexandria Engineering Journal, 54(2015) 251-261. https://doi.org/10.1016/j.aej.2015.03.003.

[117] S. R. Elkoumy, E. I. Barakat, S. I. Abdelsalam, Hall and Transverse Magnetic Field Effects on Peristaltic Flow of a Maxwell Fluid through a Porous Medium,

Global Journal of Pure and Applied Mathematics, 9(2013) 187–203. *https* : *//buescholar.bue.edu.eg/basic$_s$ci$_e$ng/*30.

[118] S. Gupta, D. Kumar, J. Singh, Analytical study for MHD flow of Williamson nanofluid with the effects of variable thickness, nonlinear thermal radiation and improved Fourier's and Fick's Laws, SN Applied Sciences, 2(2020) 1-12. https://doi.org/10.1007/s42452-020-1995-x.

[119] S. Jena, G. C. Dash, S. R. Mishra, Chemical reaction effect on MHD viscoelastic fluid flow over a vertical stretching sheet with heat source/sink, Ain Shams Engineering Journal, 9(2018) 1205-1213. https://doi.org/10.1016/j.asej.2016.06.014

[120] S. Liao, Beyond Perturbation: Introduction to the Homotopy Analysis Method, Chapman and Hall/CRC Press, (2003). http://doi.org/10.1201/9780203491164.

[121] S. Liao, Homotopy analysis method in nonlinear differential equations, Beijing: Higher education press, 2012.

[122] S. R. Mishra, I. Khan, Q. M. Al-Mdallal, T. Asifa, Free convective micropolar fluid flow and heat transfer over a shrinking sheet with heat source, Case studies in thermal engineering, 11(2018) 113-119. https://doi.org/10.1016/j.csite.2018.01.005.

[123] S. Nadeem, S. T. Hussain, C. Lee, Flow of a Williamson fluid over a stretching sheet, Brazilian journal of chemical engineering, 30(2013) 619-625. https://doi.org/10.1590/S0104-66322013000300019.

[124] S. Nadeem, R. U. Haq, C. Lee, MHD boundary layer flow over an unsteady shrinking sheet: analytical and numerical approach, Journal of the Brazilian society of Mechanical sciences and Engineering, 37(2015) 1339-1346. https://doi.org/10.1007/s40430-014-0261-9.

[125] S. R. Pradhan, S. Baag, S. R. Mishra, M. R. Acharya, Free convective MHD micropolar fluid flow with thermal radiation and radiation absorption: A numerical study, Heat Transfer—Asian Research, 48(2019) 2613-2628. https://doi.org/10.1002/htj.21517.

[126] S. Rosseland, Astrophysik und atom-theoretische Grundlagen, Springer-Verlag; Berlin, 1931.

[127] T. M. Ajayi, A. J. Omowaye, I. L. Animasaun, Effects of viscous dissipation and double stratification on MHD Casson fluid flow over a surface with variable thickness: boundary layer analysis, In International journal of engineering research in Africa, 28(2017) 73-89. https://doi.org/10.4028/www.scientific.net/JERA.28.73.

[128] T. Abbas, S. Rehman, R. Shah, M. Idrees, M. Qayyum, Analysis of MHD Carreau fluid flow over a stretching permeable sheet with variable viscosity and thermal conductivity, Physica A-statistical Mechanics and Its Applications, 551(2020) 124225. https://doi.org/10.1016/j.physa.2020.124225.

[129] T. Tayebi, A. S. Dogonchi, A. J. Chamkha, M. B. B. Hamida, S. El-Sapa, A. M. Galal, Micropolar nanofluid thermal free convection and entropy generation through an inclined I-shaped enclosure with two hot cylinders, Case Studies in Thermal Engineering, 31(2022) 101813. https://doi.org/10.1016/j.csite.2022.101813.

[130] T. A. Yusuf, F. Mabood, B. C. Prasannakumara, I. E. Sarris, Magneto-bioconvection flow of Williamson nanofluid over an inclined plate with gyrotactic microorganisms and entropy generation, Fluids, 6(2021), 109. https://doi.org/10.3390/fluids6030109.

[131] U. Ali, M. Y. Malik, A. A. Alderremy, S. Aly, K. U. Rehman, A generalized findings on thermal radiation and heat generation/absorption in nanofluid flow regime, Physica A: Statistical Mechanics and its Applications, 553(2020) 124026. https://doi.org/10.1016/j.physa.2019.124026.

[132] U. Ghosh, Electro-magneto-hydrodynamics of non-linear viscoelastic fluids, Journal of Non-Newtonian Fluid Mechanics, 277(2020) 104234. https://doi.org/10.1016/j.jnnfm.2020.104234.

[133] U. S. Mahabaleshwar, K. R. Nagaraju, M. A. Sheremet, P. N. Vinay Kumar, G. Lorenzini, Effect of mass transfer and MHD induced Navier's slip flow due to a non linear stretching sheet, Journal of Engineering Thermophysics, 28(2019) 578-590. https://doi.org/10.1134/S1810232819040131.

[134] U. Nazir, S. Saleem, M. Nawaz, M. A. Sadiq, A. Alderremy, Study of transport phenomenon in Carreau fluid using Cattaneo-Christov heat flux model with temperature dependent diffusion coefficients, Physica A: Statistical Mechanics and its Applications, 554(2020) 123921. https://doi.org/10.1016/j.physa.2019.123921.

[135] W. A. Khan, I. Pop, Boundary-layer flow of a nanofluid past a stretching sheet, International journal of heat and mass transfer, 53(2010) 2477-2483. https://doi.org/10.1016/j.ijheatmasstransfer.2010.01.032.

[136] W. Wang, B. W. Li, P. L. Varghese, X. Y. Leng, X. Y. Tian, Numerical analysis of three-dimensional MHD natural convection flow in a short horizontal cylindrical annulus, International Communications in Heat and Mass Transfer, 98(2018) 273-285. https://doi.org/10.1016/j.icheatmasstransfer.2018.09.009.

[137] W. Ibrahim, Magnetohydrodynamics (MHD) flow of a tangent hyperbolic fluid with nanoparticles past a stretching sheet with second order slip and convective boundary condition. Results in physics, 7(2017) 3723-3731. https://doi.org/10.1016/j.rinp.2017.09.041.

[138] Y. S. Daniel, Z. A. Aziz, Z. Ismail, A. Bahar, Unsteady EMHD dual stratified flow of nanofluid with slips impacts, Alexandria Engineering Journal, 59(2020) 177-189. https://doi.org/10.1016/j.aej.2019.12.020.

[139] Y. S. Daniel, Z. A. Aziz, Z. Ismail, F. Salah, Impact of thermal radiation on electrical MHD flow of nanofluid over nonlinear stretching sheet with variable thickness, Alexandria Engineering Journal, 57(2018) 2187-2197. https://doi.org/10.1016/j.aej.2017.07.007.

[140] Y. S. Daniel, Z. A. Aziz, Z. Ismail, F. Salah, Double stratification effects on unsteady electrical MHD mixed convection flow of nanofluid with viscous dissipation and Joule heating, Journal of applied research and technology, 15(2017) 464-476. https://doi.org/10.1016/j.jart.2017.05.007.

[141] Y. Lin, L. Zheng, B. Li, L. Ma, A new diffusion for laminar boundary layer flow of power law fluids past a flat surface with magnetic effect and suction or injection, International Journal of Heat and Mass Transfer, 90(2015) 1090-1097. https://doi.org/10.1016/j.ijheatmasstransfer.2015.07.067.

[142] Y. D. Reddy, B. S. Goud, A. J. Chamkha, M. A. Kumar, Influence of radiation and viscous dissipation on MHD heat transfer Casson nanofluid flow along a nonlinear stretching surface with chemical reaction, Heat Transfer, 51(2022) 3495-3511. https://doi.org/10.1002/htj.22460.

[143] Z. Li, M. Sheikholeslami, A. S. Mittal, A. Shafee, R. U. Haq, Nanofluid heat transfer in a porous duct in the presence of Lorentz forces using the lattice Boltzmann method, The European Physical Journal Plus, 134(2019) 1-10. https://doi.org/10.1140/epjp/i2019-12406-8.

[144] Z. M. Yusof, S. K. Soid, A. S. Abd Aziz, S. A. Kechil, Radiation effect on unsteady MHD flow over a stretching surface, International Journal of Computer and Information Engineering, 6(2012) 1772-1775. https://doi.org/10.5281/zenodo.1062348.